

## Discovery and optimization of small molecule splicing modifiers of survival motor neuron 2 (SMN2) as a treatment for spinal muscular atrophy

Matthew G Woll, Hongyan Qi, Anthony Turpoff, Nanjing Zhang, Xiaoyan Zhang, Guangming Chen, Chunshi Li, Song Huang, Tianle Yang, Young-Choon Moon, Chang-Sun Lee, Soongyu Choi, Neil G. Almstead, Nikolai N. Naryshkin, Amal Dakka, Jana Narasimhan, Vijayalakshmi Gabbeta, Ellen Welch, Xin Zhao, Nicole Risher, Josephine Sheedy, Marla Weetall, and Gary M. Karp

*J. Med. Chem.*, **Just Accepted Manuscript** • DOI: 10.1021/acs.jmedchem.6b00460 • Publication Date (Web): 14 Jun 2016

Downloaded from <http://pubs.acs.org> on June 15, 2016

### Just Accepted

“Just Accepted” manuscripts have been peer-reviewed and accepted for publication. They are posted online prior to technical editing, formatting for publication and author proofing. The American Chemical Society provides “Just Accepted” as a free service to the research community to expedite the dissemination of scientific material as soon as possible after acceptance. “Just Accepted” manuscripts appear in full in PDF format accompanied by an HTML abstract. “Just Accepted” manuscripts have been fully peer reviewed, but should not be considered the official version of record. They are accessible to all readers and citable by the Digital Object Identifier (DOI®). “Just Accepted” is an optional service offered to authors. Therefore, the “Just Accepted” Web site may not include all articles that will be published in the journal. After a manuscript is technically edited and formatted, it will be removed from the “Just Accepted” Web site and published as an ASAP article. Note that technical editing may introduce minor changes to the manuscript text and/or graphics which could affect content, and all legal disclaimers and ethical guidelines that apply to the journal pertain. ACS cannot be held responsible for errors or consequences arising from the use of information contained in these “Just Accepted” manuscripts.

1  
2  
3  
4  
5  
6  
7  
8  
9  
10  
11  
12  
13  
14  
15  
16  
17  
18  
19  
20  
21  
22  
23  
24  
25  
26  
27  
28  
29  
30  
31  
32  
33  
34  
35  
36  
37  
38  
39  
40  
41  
42  
43  
44  
45  
46  
47  
48  
49  
50  
51  
52  
53  
54  
55  
56  
57  
58  
59  
60

# Discovery and optimization of small molecule splicing modifiers of survival motor neuron 2 (*SMN2*) as a treatment for spinal muscular atrophy

*Matthew G. Woll, Hongyan Qi, Anthony Turpoff, Nanjing Zhang, Xiaoyan Zhang, Guangming Chen, Chunshi Li, Song Huang, Tianle Yang, Young-Choon Moon, Chang-Sun Lee, Soongyu Choi, Neil G. Almstead, Nikolai A. Naryshkin, Amal Dakka, Jana Narasimhan, Vijayalakshmi Gabbeta, Ellen Welch, Xin Zhao, Nicole Risher, Josephine Sheedy, Marla Weetall, Gary M. Karp\**

PTC Therapeutics, Inc., 100 Corporate Court, South Plainfield, NJ 07080, United States

## ABSTRACT

The underlying cause of spinal muscular atrophy (SMA) is a deficiency of the survival motor neuron (SMN) protein. Starting from hits identified in a high throughput screening campaign and through structure–activity relationship (SAR) investigations, we have developed small molecules that potently shift the alternative splicing of the *SMN2* exon 7, resulting in increased production of the full-length SMN mRNA and protein. Three novel chemical series, represented by compounds **9**, **14**, and **20**, have been optimized to increase the level of SMN protein by >50% in SMA patient–derived fibroblasts at concentrations < 160 nM. Daily administration of these compounds to severe SMA  $\Delta 7$  mice results in an increased production of SMN protein in disease relevant tissues and a significant increase in median survival time in a dose dependent manner.

1  
2  
3 Our work supports the development of an orally administered small molecule for the treatment of  
4 patients with SMA.  
5  
6

## 7 8 9 INTRODUCTION

10  
11 Spinal muscular atrophy (SMA) is caused by a genetic defect in the *SMN1* gene, rendering it  
12 incapable of producing the survival motor neuron protein (SMN).<sup>1,2</sup> Humans usually have two  
13 or more copies of the paralogous *SMN2* gene, but this gene produces much less functional SMN  
14 protein due to an alternative splicing event of exon 7. This alternative pathway is the result of a  
15 translationally synonymous C to T mutation in exon 7. As a result, the majority of transcripts  
16 produced from *SMN2* lack exon 7 (*SMN2-Δ7*), and encode a truncated SMN-Δ7 protein that is  
17 rapidly degraded.<sup>3,4</sup>  
18  
19  
20  
21  
22  
23  
24  
25  
26  
27

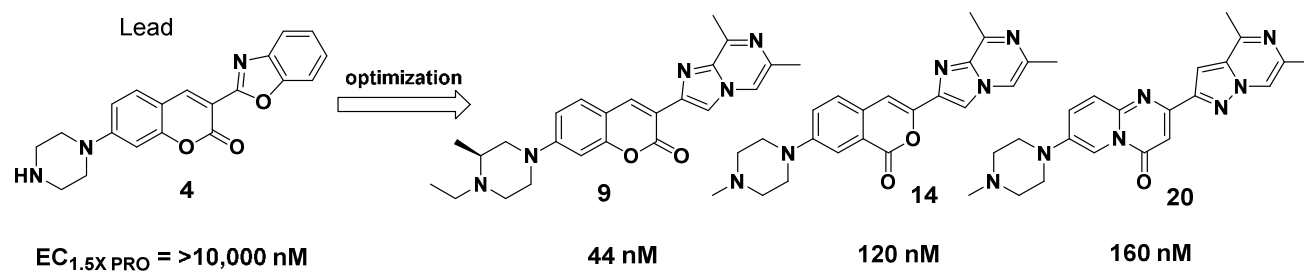
28  
29 Antisense oligonucleotides (ASOs) that target the ISS-N1 regulatory element near exon 7 of  
30 *SMN2* pre-mRNA can shift the outcome of the splicing reaction toward the generation of full  
31 length *SMN2* mRNA.<sup>5-7</sup> Initial reports with 2'-O-methoxy-ethyl ribose (MOE) phosphorothioate  
32 ASOs that were delivered by intracerebroventricular (ICV) injection to neonatal mice with a  
33 severe SMA phenotype at postnatal day 1 (PND1) produced an increase in SMN protein levels in  
34 neuronal tissue, but only modestly increased the median survival time of the mice.<sup>8</sup> In order to  
35 achieve maximum survival benefit, co-administration of the ASO via subcutaneous (SC)  
36 injection was required.<sup>9</sup> Phosphorodiamidate morpholino oligonucleotides (PMOs) targeting ISS-  
37 N1 demonstrated a much greater survival benefit than MOE ASOs after a single ICV injection.<sup>10-</sup>  
38  
39  
40  
41  
42  
43  
44  
45  
46  
47  
48  
49  
50  
51  
52  
53  
54  
55  
56  
57  
58  
59  
60

1  
2  
3 Despite the promising results of the ASOs, there remained a need to discover and develop  
4  
5 compounds with improved activity and pharmaceutical properties. Small molecules possess the  
6  
7 inherent advantage of oral administration and broad peripheral and CNS distribution. Several  
8  
9 classes of small molecules (e.g., hydroxyurea, salbutamol, tetracycline derivatives) have been  
10  
11 reported to modify the alternative splicing of *SMN2* exon 7.<sup>14-20</sup> However, the biological activity  
12  
13 of all these compounds is weak compared to that of ASOs. We recently disclosed the structures  
14  
15 of three small molecules that shift *SMN2* splicing toward the production of full-length *SMN2*  
16  
17 mRNA with high selectivity.<sup>21</sup> Administration of these compounds to SMA mice led to an  
18  
19 increase in SMN protein levels, improvement of motor function, protection of the neuromuscular  
20  
21 circuit, and an extended life span. Recently, another series of small molecules demonstrated a  
22  
23 long term survival benefit in SMA mice.<sup>22</sup> The compounds were shown to enhance the  
24  
25 recruitment of the U1 snRNP to the (non-canonical) 5' splice site in *SMN2* intron 7. Our  
26  
27 compounds similarly enhance the U1 – pre-mRNA interaction at the 5' splice site of *SMN2*  
28  
29 intron 7.  
30  
31  
32  
33  
34  
35  
36

37 Herein we describe the discovery and chemical optimization of the three chemical series  
38  
39 disclosed in our previous publication.<sup>21</sup> Through chemical modification of hits identified in a  
40  
41 high throughput screen of our chemical library, we identified molecules that demonstrate both an  
42  
43 increase in the full length *SMN2* transcript (*SMN-FL*) and a concomitant decrease in *SMN2-Δ7*.  
44  
45 A detailed structure–activity relationship (SAR) investigation improved the potency of the lead  
46  
47 molecules nearly three orders of magnitude (Figure 1). Increases in the level of full-length *SMN2*  
48  
49 mRNA resulted in significantly increased SMN protein levels in SMA patient–derived cells and  
50  
51 in mice with a severe SMA phenotype ( $\Delta 7$  mice). Moreover, as a consequence of the increased  
52  
53  
54  
55  
56  
57  
58  
59  
60

level of SMN protein, administration of these compounds significantly prolongs survival in  $\Delta 7$  mice.

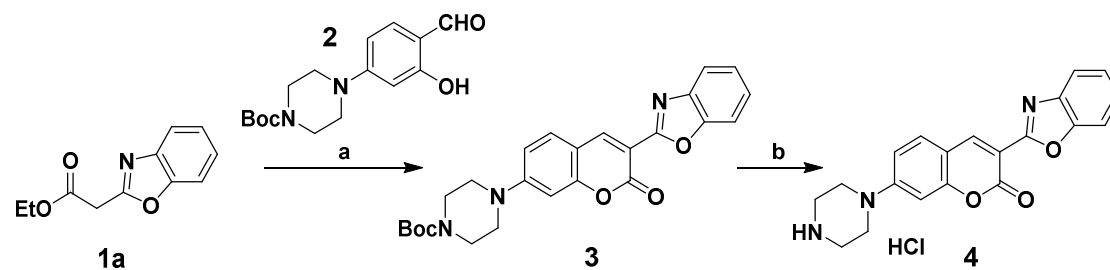
**Figure 1.** Three novel chemical series discovered in lead optimization



## RESULTS AND DISCUSSION

**Chemistry.** In order to synthesize various 3,7-disubstituted coumarins, an appropriately substituted ethyl 2-aryl/heteroaryl-acetate (**1a** for 3-benzoxazolyl coumarins) can undergo aldol condensation with an appropriately substituted salicylaldehyde (**2** for 7-piperazinyl coumarins). The transient condensation product undergoes ring-closing transesterification to give coumarin **3**, as shown in Scheme 1. Removal of the Boc protecting group with hydrogen chloride in 1,4-dioxane provides **4**.

**Scheme 1.** The synthesis of 3,7-disubstituted coumarin **4**<sup>a</sup>

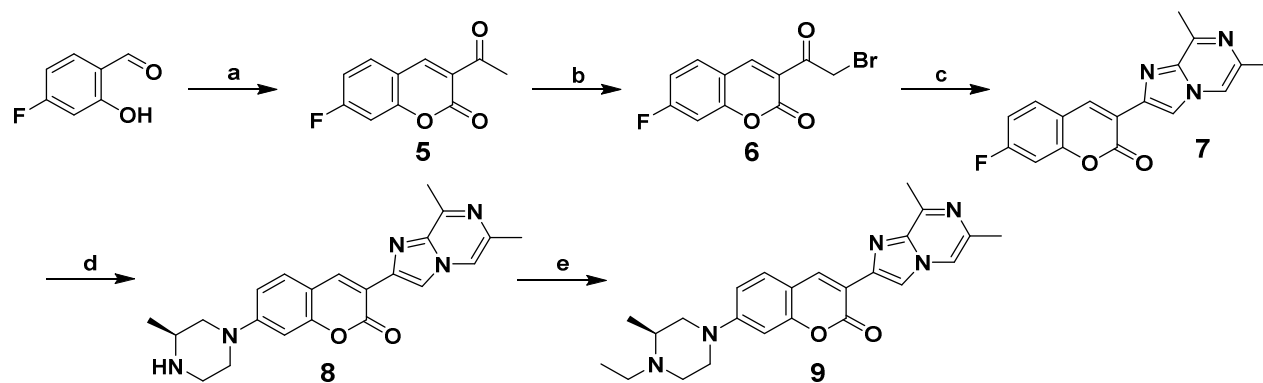


1  
2  
3  
4  
5  
6  
7  
8  
9  
10  
11  
12  
13  
14  
15  
16  
17  
18  
19  
20  
21  
22  
23  
24  
25  
26  
27  
28  
29  
30  
31  
32  
33  
34  
35  
36  
37  
38  
39  
40  
41  
42  
43  
44  
45  
46  
47  
48  
49  
50  
51  
52  
53  
54  
55  
56  
57  
58  
59  
60

<sup>a</sup>Conditions: (a) **2** (1.05 equiv), piperidine (0.25 equiv), AcOH (0.1 equiv), EtOH, reflux, 24 h, 93%; (b) 4 N HCl in 1,4-dioxane, rt, 3 h, 85%.

An alternative strategy to generate 3,7-disubstituted coumarins, when it is desired to fix the 3-position as a specific imidazo-heterocycle, can be found in Scheme 2. Aldol condensation of ethyl acetoacetate with 4-fluorosalicylaldehyde, followed by ring-closing transesterification yields coumarin **5**. Treatment of **5** with bromine provides the  $\alpha$ -bromoketone **6**. When **6** and 2-amino-3,5-dimethylpyrazine are combined at elevated temperatures, an alkylation-condensation reaction occurs to generate **7**. The nucleophilic displacement of fluorine at the 7-position of **7** by (*S*)-2-methylpiperazine provides **8**. A diverse set of amines can be introduced at this stage of the synthesis. Additional diversification of **8** was achieved through reductive amination or alkylation of the secondary amine. The *N*-ethyl variant **9** was obtained after treatment of **8** with acetaldehyde and sodium triacetoxyborohydride.

**Scheme 2.** The synthesis of 3,7-disubstituted coumarin **9**<sup>a</sup>

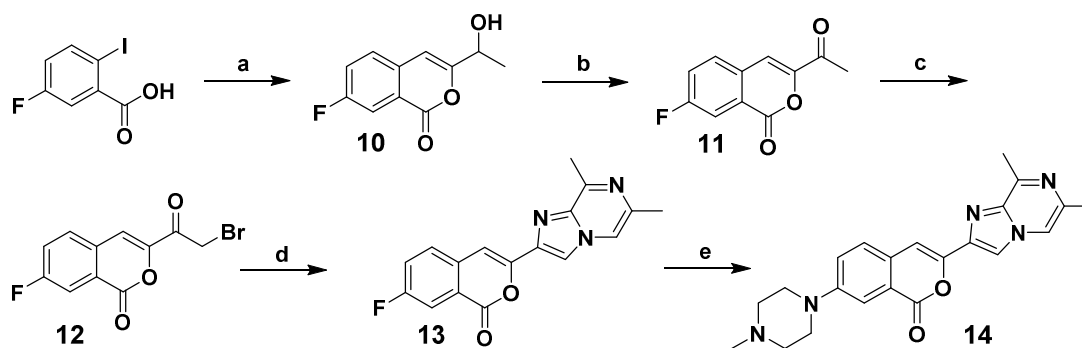


<sup>a</sup>Conditions: (a) ethyl acetoacetate (1 equiv), piperidine (0.1 equiv), rt, 10 min, 95%; (b) Br<sub>2</sub> (1.05 equiv), CHCl<sub>3</sub>, rt, 1 h, 72%; (c) 2-amino-3,5-dimethylpyrazine (0.85 equiv), CH<sub>3</sub>CN, 120

°C, 20 min, 90%; (d) (*S*)-2-methylpiperazine (2.1 equiv), K<sub>2</sub>CO<sub>3</sub> (4 equiv), DMSO, 120 °C, 2 h, 64%; (e) CH<sub>3</sub>CHO (2 equiv), NaBH(OAc)<sub>3</sub> (3 equiv), CH<sub>2</sub>Cl<sub>2</sub>:MeOH (9:1), rt, 16 h, 72%.

Using a similar synthetic strategy as found in Scheme 2, isocoumarins could be generated from intermediate **12** (Scheme 3). The generation of the isocoumarin core, however, required a distinct synthetic pathway from the coumarins. The lactone architecture was generated via a Sonogashira coupling of 3-butyn-2-ol to 2-iodo-5-fluoro-benzoic acid. Under the reaction conditions, the alkyne intermediate undergoes nucleophilic attack by the ortho-carboxylate, giving isocoumarin **10**. Oxidation of **10** with manganese (IV) oxide gives methyl ketone **11**, which can be brominated alpha to the ketone to give **12**. Intermediate **12** was converted to **14** in a similar fashion as found in Scheme 2. Interestingly, the treatment of **13** with 1-methyl-piperazine leads initially to lactone ring opening. Next, the fluorine on the ring-opened intermediate is displaced by an additional 1-methyl-piperazine molecule. Finally, the isocoumarin lactone ring reforms and subsequently remains intact, due to the increased stability provided by the electron donating amine.

**Scheme 3.** The synthesis of 3,7-disubstituted isocoumarin **14**<sup>a</sup>

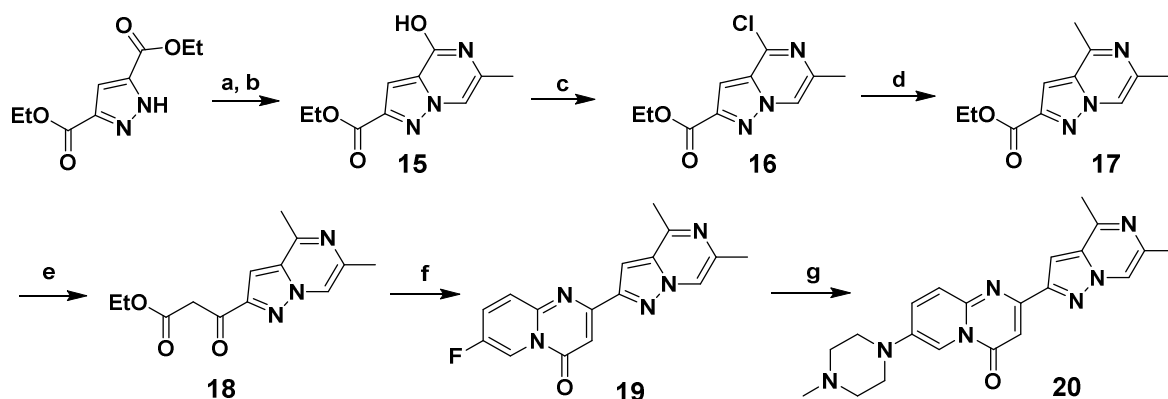


<sup>a</sup>Conditions: (a) 3-butyn-2-ol (2.3 equiv), ZnCl<sub>2</sub> (1 equiv), Pd(PPh<sub>3</sub>)<sub>4</sub> (0.05 equiv), Et<sub>3</sub>N (3 equiv), DMF, 100 °C, 2 h, 84% ; (b) MnO<sub>2</sub> (10 equiv), CH<sub>2</sub>Cl<sub>2</sub>, rt, 48 h, 66%; (c) Br<sub>2</sub> (1.1 equiv),

CHCl<sub>3</sub>, rt, 1 h, 96%; (d) 2-amino-3,5-dimethylpyrazine (1.1 equiv), CH<sub>3</sub>CN, 100 °C, 16 h, 93%;  
 (e) 1-methyl-piperazine (3 equiv), NMP, 180 °C, 24 h, 57%.

Access to 2,7-disubstituted pyridopyrimidinones required a different synthetic approach than the previously described routes for coumarins and isocoumarins. Diversity is achieved by condensing ethyl β-ketoaryl esters (e.g. **18**) with 2-amino-5-fluoropyridine to generate **19** as depicted in Scheme 4. The fluorine at the 7-position in **19** can undergo nucleophilic displacement with amines as described in previous Schemes to give **20**. Access to intermediate **18** begins with the tandem alkylation-condensation reaction of diethyl 1H-pyrazole-3,5-dicarboxylate with chloroacetone in the presence of ammonium acetate to provide **15**. The 4-hydroxyl group of **15** can be converted to chlorine in high yield with phosphorus oxychloride. A Suzuki coupling using methanoboronic acid converts the chlorine to methyl (**17**). Claisen condensation with *tert*-butyl acetate provides a *tert*-butyl-β-keto-intermediate that is transformed to **18** via transesterification in ethanol.

**Scheme 4.** The synthesis of 2,7-disubstituted pyridopyrimidinone **20**<sup>a</sup>



<sup>a</sup>Conditions: (a) chloroacetone (1 equiv), K<sub>2</sub>CO<sub>3</sub> (1.1 equiv), acetone, 30 °C, 6.5 h; (b) NH<sub>4</sub>OAc (20 equiv), AcOH, reflux, 60 h, 64% over 2 steps; (c) POCl<sub>3</sub>, reflux, 16 h, 85%; (d) MeB(OH)<sub>2</sub>

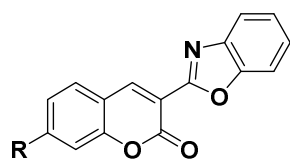
1  
2  
3 (3 equiv), Pd(PPh<sub>3</sub>)<sub>4</sub> (0.03 equiv), K<sub>2</sub>CO<sub>3</sub> (5 equiv), DMF, 100 °C, 15 h, 82%; (e) i) *tert*-  
4  
5 butylacetate (2 equiv), LDA (2.4 equiv), -78 °C to -30 °C, 97%, ii) EtOH, 120 °C, 1 h, 98%; (f)  
6  
7  
8 2-amino-5-fluoropyridine (1.2 equiv), pyridinium *p*-toluenesulfonate (0.05 equiv), 130 °C, 8 h,  
9  
10 71%; (g) 1-methyl-piperazine (10 equiv), DMAc, 120 °C, 15 h, 80%.

11  
12  
13  
14 **HTS and lead discovery.** In order to identify compounds that increase the inclusion of exon 7  
15  
16 during *SMN2* pre-mRNA splicing, a HEK293H cell line was generated that contained an *SMN2*  
17  
18 gene fragment (from exon 6 to the 5' region of exon 8), followed by the firefly luciferase coding  
19  
20 sequence. Luciferase is expressed only when splicing includes *SMN2* exon 7 in the mRNA,  
21  
22 otherwise the luciferase coding sequence is out of the translational reading frame with respect to  
23  
24 the initiation codon upstream of the *SMN2* sequence. The ratio of the *SMN2-Δ7* transcript to the  
25  
26 *SMN2-FL* transcript in this minigene construct is ~97:3. Full correction of splicing would result  
27  
28 in a ~30-fold increase in the *SMN2-FL* transcript. In the type 1 SMA patient-derived fibroblasts  
29  
30 (GM03813) the ratio of the *SMN2-Δ7* transcript to the *SMN2-FL* transcript is ~1:1. We reasoned  
31  
32 that screening compounds using the minigene construct could be advantageous as the larger  
33  
34 dynamic range in the minigene assay would allow for the identification of compounds with weak  
35  
36 activity. Using the minigene assay to screen our library of ~200,000 compounds, we identified  
37  
38 molecules that increased the luciferase signal more than 3-fold above the DMSO control level.  
39  
40 All compounds identified in the primary screen were confirmed in the minigene assay for  
41  
42 concentration-response activity by measuring the relative amount of *SMN2-FL* mRNA using the  
43  
44 reverse transcription-quantitative polymerase chain reaction (RT-qPCR). Compounds were  
45  
46 compared by measuring the concentration required to increase the amount of *SMN2-FL* to a level  
47  
48 1.5 fold that of the baseline (EC<sub>1.5X RNA</sub>). Several hits were identified for further evaluation.  
49  
50  
51  
52  
53  
54  
55  
56  
57  
58  
59  
60

1  
2  
3 For each hit we designed dozens of structurally similar analogs in an effort to establish a  
4 structure–activity relationship (SAR) and identify a lead series to optimize for development. A  
5 coumarin hit (**21**) showed promising activity ( $EC_{1.5X\ RNA} = 0.22\ \mu\text{M}$ ). Several analogs of **21** were  
6 synthesized by modifying the 7-position of the coumarin, exchanging the diethylamino  
7 substituent with structurally similar moieties. Upon initial inspection it appeared problematic to  
8 make even minor structural modifications at the 7-position without negatively impacting activity  
9 (Table 1, compounds **4**, **22–24**). We observed that analog **4**, containing a piperazine at the 7-  
10 position, induced a maximum amount of *SMN2-FL* (max fold RNA) that was much greater than  
11 that induced by the other analogs, even though the compound had an  $EC_{1.5X\ RNA}$  considerably  
12 lower than that of **21**.  
13  
14  
15  
16  
17  
18  
19  
20  
21  
22  
23  
24  
25  
26  
27

28 Further insight was achieved when we evaluated the  $EC_{1.5X\ RNA}$  without normalization to  
29 GAPDH mRNA (a standard reference mRNA). Although GAPDH normalization is used to  
30 remove some of the artifacts of PCR amplification, it can produce an artificially high increase in  
31 the mRNA of interest in cases when GAPDH mRNA decreases at a relative rate greater than that  
32 of the mRNA of interest. (This phenomenon may occur at concentrations at which the compound  
33 exhibits cytotoxicity). Analysis of the *SMN2-FL* data without GAPDH correction (Table 1, Not  
34 GAPDH normalized) showed that compound **21** was weakly active, whereas **4** retained  
35 substantial activity. Based on these data, we reasoned that the basic amine found in **4** was a  
36 critical component of the pharmacophore and focused our efforts on synthesizing additional 7-  
37 piperazino coumarin analogs.  
38  
39  
40  
41  
42  
43  
44  
45  
46  
47  
48  
49  
50  
51  
52

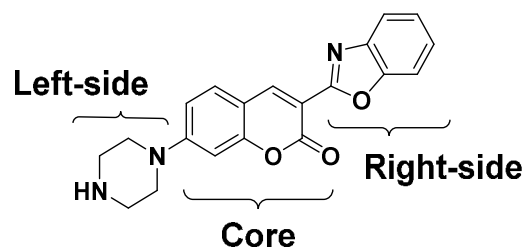
53 **Table 1.** *In vitro* activity of 7-substituted coumarins in the SMN2 minigene assay  
54  
55  
56  
57  
58  
59  
60



Compd	R	GAPDH normalized		Not GAPDH normalized	
		EC <sub>1.5x RNA</sub> (μM)	Max fold	EC <sub>1.5x RNA</sub> (μM)	Max fold
21		0.22	4.5	>32	1.2
22		22	1.5	>32	1.2
23		>32	1.0	>32	1.0
24		>32	1.0	>32	1.1
4		8.7	25	10	7

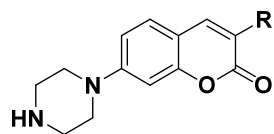
**Lead optimization.** Although compound **4** increased *SMN2-FL* levels in the minigene assay, its potency was modest (EC<sub>1.5x RNA</sub> ~ 10 μM). Additionally, compound **4** did not induce a measurable increase in the level of SMN protein in SMA patient-derived fibroblasts, likely due to its weak activity.<sup>23</sup> We pursued potency improvements by modifying the three heterocyclic constituents of the molecule. For the purpose of clarity we adopted the nomenclature shown in Figure 2. The coumarin moiety is referred to as the “core”, which is flanked on the “left-side” by the basic piperazine moiety and on the “right-side” by the benzoxazole.

**Figure 2.** Nomenclature for the three heterocyclic constituents of **4**

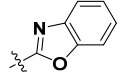
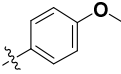
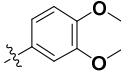
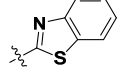
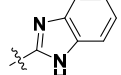
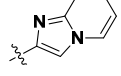
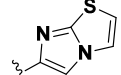


Initial gains in potency were achieved by modifying the right-side heterocycle.<sup>24</sup> Replacing the benzoxazole ring with phenyl (**25**) resulted in loss of activity, but phenyl rings substituted with electron donating groups (**26** and **27**) resulted in increased potency in the minigene assay (Table 2). Compound **27** showed a modest but clearly measurable 1.3-fold increase in the level of SMN protein; however, no additional improvement could be achieved with other substituted phenyl groups (data not shown). We then focused our attention toward replacing the benzoxazole with novel heterocycles. Improvement of potency in the minigene assay was achieved by replacing the benzoxazole with benzothiazole (**28**). Further improvement was achieved with benzimidazole **29** and constitutionally isomeric imidazopyridine **30**. Replacing the pyridine ring in imidazopyridine **30** with a thiazole ring gave the more potent imidazothiazole **31**, with an  $EC_{1.5X}$  RNA of 0.11  $\mu$ M. Compound **31** was the first compound identified to achieve a >1.5 fold increase in SMN protein as measured in SMA patient-derived fibroblasts ( $EC_{1.5X}^{PRO} = 0.36 \mu$ M).

**Table 2.** *In vitro* activity of 3-substituted coumarins



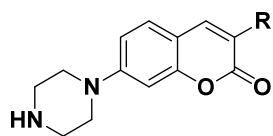
Compd	R	RNA minigene	SMN protein	
		$EC_{1.5X}^{RNA}$ ( $\mu$ M)	$EC_{1.5X}^{PRO}$ ( $\mu$ M)	Max fold

4		8.7	>10	1.0
25		>32	>10	1.0
26		2.0	>10	1.1
27		0.62	>10	1.3
28		1.0	>10	1.0
29		0.43	>10	1.2
30		0.38	>10	1.3
31		0.11	0.36	1.5

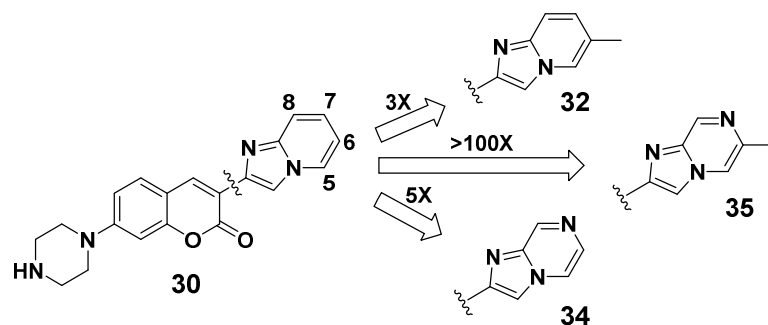
We next extended our SAR investigation by evaluating the effect of substitution on the imidazopyridine ring in compound **30**. The  $EC_{1.5X\ RNA}$  of 380 nM for **30** was improved ~3-fold by appending a methyl group to the 6-position of the imidazopyridine in **32** (Table 3). Substitution with the larger 6-ethyl group (**33**), however, was detrimental to potency. A modest 5-fold gain in potency could also be achieved by replacing C7 of the heterocycle with a nitrogen atom to afford the imidazopyrazine **34**. Combining the 6-methyl substituent with the C-7 nitrogen of the imidazopyrazine (**35**) resulted in a dramatic >100-fold improvement in potency ( $EC_{1.5X\ RNA} = 2\text{ nM}$ ), demonstrating an effect often encountered in drug discovery whereby two small structural modifications, each alone producing a minor improvement in activity, but together imparting a profound effect on activity. This cooperative enhancement was observed when making modifications to the imidazopyridine series (Figure 3). The dramatic improvement

in potency observed in the minigene assay in **35** ( $EC_{1.5X\ RNA} = 2\text{ nM}$ ) was also observed in SMA patient-derived fibroblasts ( $EC_{1.5X\ PRO} = 5\text{ nM}$ ). Further investigation revealed that the 8-position of the imidazopyrazine could tolerate methyl substitution (**36**), but larger groups such as ethyl (**37**) led to diminished potency. The 8-Me modification was incorporated into the structure of many subsequent molecules, despite the 3-fold loss in potency, due to a beneficial gain in plasma and tissue exposure in mice and rats (further described in the pharmacokinetics section).

**Table 3.** *In vitro* activity of 3-substituted coumarins (imidazo-heterocycles)

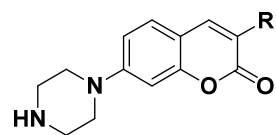


Compd	R	RNA minigene $EC_{1.5X\ RNA}$ (nM)	SMN protein $EC_{1.5X\ PRO}$ (nM)
<b>30</b>		380	>10,000
<b>32</b>		140	160
<b>33</b>		2700	>10,000
<b>34</b>		70	120
<b>35</b>		2	5
<b>36</b>		2	15
<b>37</b>		10	210

**Figure 3.** Cooperative potency enhancement of the nitrogen-methyl pair

Additional heterocyclic-containing coumarin analogs having the Me/N pairing found in the most active imidazopyrazines were synthesized (Table 4). Several of the compounds were very active (**38-40**,  $EC_{1.5X\ PRO} < 100$  nM) while others were nearly inactive (**41-42**,  $EC_{1.5X\ PRO} > 10,000$  nM).

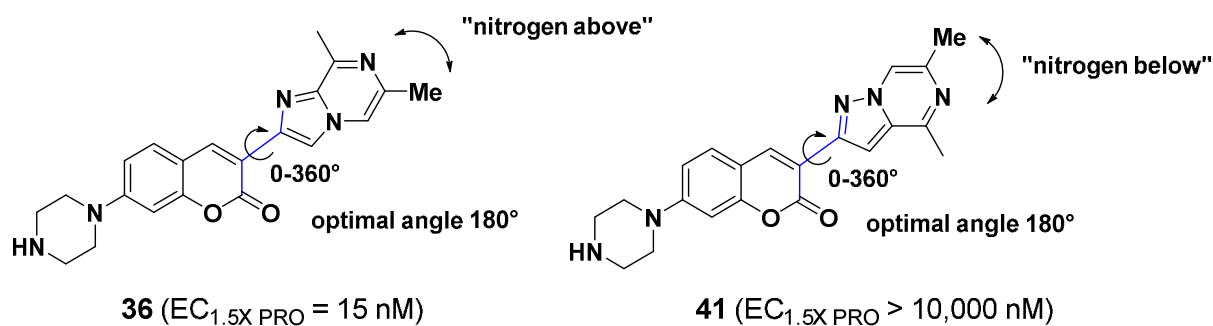
It became apparent that the relative orientation of the Me/N pharmacophore with respect to the coumarin is important (Figure 4). For example, when the relative energy for rotation about the coumarin-imidazopyrazine bond (e.g., **36**) is calculated, the lowest energy conformation gives a dihedral angle of  $180^\circ$  (see supplemental Graph 1). In this planar orientation the key nitrogen is located above the key methyl as drawn in Figure 4. When the heterocycle is modified to pyrazolopyrazine **41**, the  $180^\circ$  dihedral angle is still highly favored, but the key nitrogen is located below the key methyl when drawn in a similar planar fashion. Compounds containing heterocycles that favor (or do not strongly disfavor) the “nitrogen above” orientation are highly potent, while compounds that highly favor the “nitrogen below” orientation are nearly inactive.

**Table 4.** *In vitro* activity of 3-substituted coumarins

Compd	R	RNA minigene EC <sub>1.5X RNA</sub> (nM)	SMN protein EC <sub>1.5X PRO</sub> (nM)
36		2	15
38		4	16
39		4	29
40		5	66
41*		>10,000	>10,000
42		1500	>10,000

\*Left-side heterocycle is N-Me-piperidine, instead of piperazine (see Table 5 for activity comparison).

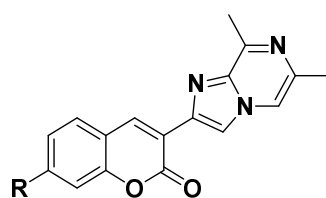
**Figure 4.** Orientation of N/Me pair in select heterocycles

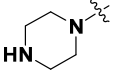
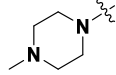
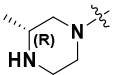
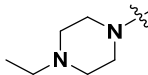
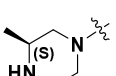
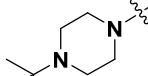
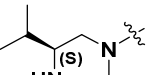
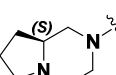
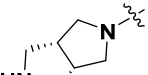
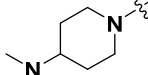
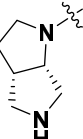
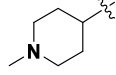
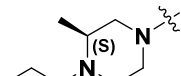
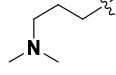
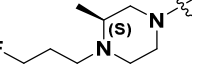


After identifying the optimized right-side heterocycles, we focused our attention on the left-side heterocycle. Earlier investigation revealed the importance of a basic amine, but did not address the optimization of amine location,  $pK_a$  or neighboring group effect. We decided to use the

1  
2  
3 highly potent unsubstituted piperazine **36** ( $EC_{1.5X\ PRO} = 15\text{ nM}$ ) as a starting point for  
4  
5 comparison. Methyl substitution at the 3-position of piperazine (e.g., **43** and **8**) typically  
6  
7 provided a modest boost to potency regardless of the absolute configuration (Table 5). A  
8  
9 decrease in potency was observed with groups larger than methyl at the 3-position (e.g.,  
10  
11 isopropyl **44**). Alkylation of the piperazine nitrogen (**49-51**) diminished potency with increasing  
12  
13 substituent size. Several additional modifications to the piperazine ring, where the basic amine  
14  
15 functionality was retained, were investigated. The ring-fused piperazine **52**, the 4'-  
16  
17 dimethylaminopiperidine **53**, and the N-methylpiperidine **54** had comparable potency in SMA  
18  
19 patient-derived fibroblasts ( $EC_{1.5X\ PRO} = 50\text{--}66\text{ nM}$ ), being only slightly less potent than the N-  
20  
21 methylpiperazine **49**. Acyclic amines were generally less potent than cyclic amines (cf.  
22  
23 compounds **54** vs. **55**). Some cyclic amine configurations were detrimental to activity, as  
24  
25 evidenced by comparing the pyrrolidinopyrrolidines **45** vs. **46**. In general,  $pK_a$  of the basic amine  
26  
27 above 7 is required to maintain activity, as demonstrated by the diminished activity of  
28  
29 fluorinated analog **47** ( $pK_a = 6.3$ ) compared to that of **48** ( $pK_a = 7.5$ ).<sup>25</sup> Although our  
30  
31 investigation of numerous heterocyclic amine-containing moieties revealed the difficulty in  
32  
33 identifying compounds with greater potency than that of those containing an unsubstituted  
34  
35 piperazine, e.g., **36**, our understanding of the tolerated modifications was important in optimizing  
36  
37 the pharmacokinetic properties of the compounds.  
38  
39  
40  
41  
42  
43  
44  
45  
46

47 **Table 5.** *In vitro* activity of 7-substituted coumarins



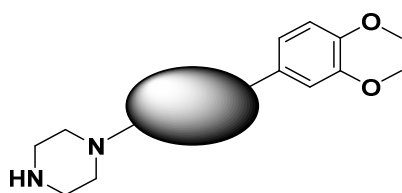
Compd	R	EC <sub>1.5X RNA</sub> (nM)	EC <sub>1.5X PRO</sub> (nM)	Compd	R	EC <sub>1.5X RNA</sub> (nM)	EC <sub>1.5X PRO</sub> (nM)
36		2	15	49		18	31
43		3	13	50		10	62
8		1	5	51		59	>10,000
44		23	76	52		21	66
45		1	13	53		11	61
46		28	640	54		11	50
47		37	450	55		58	220
48		19	60				

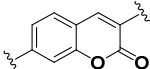
In parallel with our efforts to optimize the right- and left-sides of the coumarin lead, we began exploring alternative cores. Our initial objectives were to identify cores with improved potency and to seek cores lacking the potential liabilities inherent in coumarins.<sup>26-28</sup> Our earlier work indicated that the right- and left-side moieties had to extend from the 3- and 7-positions of the coumarin, respectively. We attempted to maintain the same spatial orientation when replacing the coumarin with other 6,6-bicyclic heterocycles. To simplify the comparison, the right-side was fixed as 3,4-dimethoxyphenyl, since this moiety showed promising activity in the coumarin

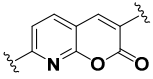
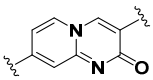
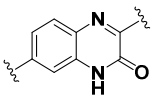
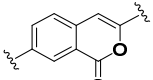
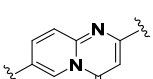
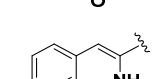
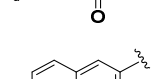
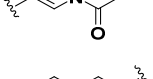
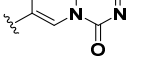
series (Table 2) and would be easily installed synthetically onto various cores. The left-side was fixed as piperazine.

We generated a variety of 6,6-heterocycles that incorporated nitrogen atoms in the core and contained a carbonyl group in the same position found in coumarin **27**, but these analogs resulted in decreased activity (Table 6, compounds **56-58**). Improvement could be achieved, however, by shifting the carbonyl group one position on the core as demonstrated by isocoumarin **59** ( $EC_{1.5X}^{RNA} = 80$  nM). One aza variation of this theme, pyridopyrimidinone **60** ( $EC_{1.5X}^{RNA} = 120$  nM), also showed improved activity compared to that of **27** ( $EC_{1.5X}^{RNA} = 620$  nM). Additional aza variations were less promising (**61-63**), as was pyridopyrimidinone **64**, in which the orientations of the piperazine and dimethoxyphenyl moieties around the pyridopyrimidinone were altered. Overall, the treatment of SMA patient-derived fibroblasts with isocoumarin **59** and pyridopyrimidinone **60** resulted in increased production of SMN protein with improved potency ( $EC_{1.5X}^{PRO} = 290$  and 830 nM, respectively) compared to that of coumarin **27** ( $EC_{1.5X}^{PRO} = >10,000$  nM).

**Table 6.** *In vitro* activity of analogs with modified cores



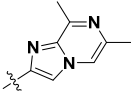
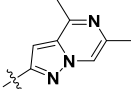
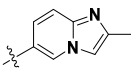
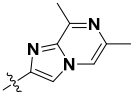
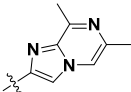
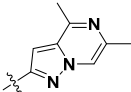
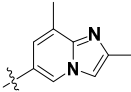
Compd		RNA minigene		SMN protein	
		$EC_{1.5X}^{RNA}$ (nM)	$EC_{1.5X}^{PRO}$ (nM)	$EC_{1.5X}^{PRO}$ (nM)	Max fold
<b>27</b>		620	>10,000	>10,000	1.3

1					
2					
3					
4	<b>56</b>		8800	>10,000	1.0
5					
6					
7	<b>57</b>		>10,000	>10,000	1.0
8					
9					
10	<b>58</b>		2200	>10,000	1.1
11					
12					
13	<b>59</b>		80	290	1.6
14					
15					
16	<b>60</b>		120	830	1.6
17					
18					
19	<b>61</b>		1400	>10,000	1.2
20					
21					
22	<b>62</b>		920	2500	1.6
23					
24					
25	<b>63</b>		>10,000	>10,000	1.0
26					
27					
28	<b>64</b>		3200	>10,000	1.0
29					
30					
31					
32					
33					
34					
35					
36	<hr/>				
37					
38					
39	Based on the activity of the isocoumarin <b>59</b> and the pyridopyrimidinone <b>60</b> we decided to				
40	synthesize additional analogs in these series incorporating several of the right-side heterocycles				
41	that were investigated in the coumarin series (Table 7). The imidazopyrazine moiety that was				
42	optimal in the coumarin series was also highly active in the isocoumarin series ( <b>65</b> , $EC_{1.5X\ PRO} =$				
43	39 nM). When the imidazopyrazine was incorporated into pyridopyrimidinone <b>66</b> , greatly				
44	diminished activity ( $EC_{1.5X\ PRO} = 430$ nM) was observed compared to that of coumarin <b>36</b>				
45	( $EC_{1.5X\ PRO} = 15$ nM). In contrast, pyridopyrimidinone <b>67</b> , which contains the pyrazolopyrazine				
46	right-side moiety, was highly active ( $EC_{1.5X\ PRO} = 31$ nM) in comparison to the corresponding				
47					
48					
49					
50					
51					
52					
53					
54					
55					
56					
57					
58					
59					
60					

Based on the activity of the isocoumarin **59** and the pyridopyrimidinone **60** we decided to synthesize additional analogs in these series incorporating several of the right-side heterocycles that were investigated in the coumarin series (Table 7). The imidazopyrazine moiety that was optimal in the coumarin series was also highly active in the isocoumarin series (**65**,  $EC_{1.5X\ PRO} = 39$  nM). When the imidazopyrazine was incorporated into pyridopyrimidinone **66**, greatly diminished activity ( $EC_{1.5X\ PRO} = 430$  nM) was observed compared to that of coumarin **36** ( $EC_{1.5X\ PRO} = 15$  nM). In contrast, pyridopyrimidinone **67**, which contains the pyrazolopyrazine right-side moiety, was highly active ( $EC_{1.5X\ PRO} = 31$  nM) in comparison to the corresponding

coumarin **41** ( $EC_{1.5X\ PRO} = >10,000$  nM). This observation is consistent with the hypothesis regarding conformation of the N/Me pair as presented in Figure 4. The lowest energy conformation gives pyrazolopyrazine **67** the “nitrogen above” orientation and imidazopyrazine **66** the “nitrogen below” orientation, a trend opposite of the one seen in the coumarin series. When the right-side heterocycle is imidazopyridine (e.g., **40** and **68**) there is no preference for the “nitrogen above” or “nitrogen below” orientation. In this case the coumarin **40** ( $EC_{1.5X\ PRO} = 66$  nM) and pyridopyrimidinone **68** ( $EC_{1.5X\ PRO} = 60$  nM) have a similar level of activity.

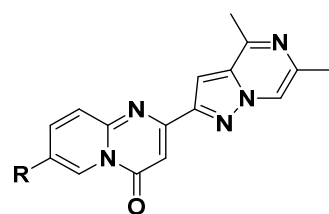
**Table 7.** *In vitro* activity of isocoumarins and pyridopyrimidinones

Compd	R	$EC_{1.5X\ RNA}$ (nM)	$EC_{1.5X\ PRO}$ (nM)
<b>36</b>		2	15
<b>41*</b>		>10,000	>10,000
<b>40</b>		5	66
<b>65</b>		8	39
<b>66</b>		180	430
<b>67</b>		6	31
<b>68</b>		48	60

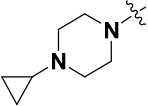
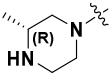
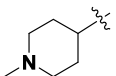
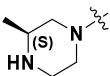
\*Left-side heterocycle is N-Me-piperidine, instead of piperazine (see Table 5 for activity comparison).

The optimal pyridopyrimidinone **67** was intriguing to us because it contained both core and right-side pieces that were structurally distinct from the optimal coumarins. We synthesized various analogs of **67** that contained alternative left-side heterocycles to determine if the same trends found in the coumarin series applied to the pyridopyrimidinone series (Table 8). Similar to the coumarins, *N*-alkylation of the piperazine reduced activity in the pyridopyrimidinones, with larger alkyl groups causing greater loss of activity (e.g., **20** and **69**). Also, similar to the coumarins, piperidine **70**, ring-fused piperazine **71**, and 4'-dimethylaminopiperidine **72** had comparable activity ( $EC_{1.5X\ PRO} = 130\text{--}210\text{ nM}$ ) to N-methylpiperazine **20** ( $EC_{1.5X\ PRO} = 170\text{ nM}$ ). In contrast to the coumarin series, incorporating 3-methyl substitution (*R* or *S*) into the piperazine ring of **67** resulted in reduced activity, with 3-(*S*)-methyl piperazine **74** ( $EC_{1.5X\ PRO} = 160\text{ nM}$ ) showing a greater loss than 3-(*R*)-methyl piperazine **73** ( $EC_{1.5X\ PRO} = 70\text{ nM}$ ).

**Table 8.** *In vitro* activity of 7-substituted pyridopyrimidinones



Compd	R	$EC_{1.5X\ RNA}$ (nM)	$EC_{1.5X\ PRO}$ (nM)	Compd	R	$EC_{1.5X\ RNA}$ (nM)	$EC_{1.5X\ PRO}$ (nM)
<b>67</b>		6	31	<b>71</b>		120	150
<b>20</b>		35	170	<b>72</b>		20	130

69		380	690	73		11	71
70		53	210	74		19	160

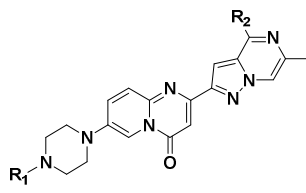
**Pharmacokinetics.** The goal of this program was to identify orally deliverable small molecule therapeutics that correct alternative splicing of the *SMN2* gene exon 7 to address the underlying cause of SMA. To identify which compounds warranted further advancement, we evaluated compounds with sufficient in vitro potency for their pharmacokinetic profile in rats. We measured plasma drug levels of test compounds at several time points up to 6 h post dose and total brain concentration at 6 h after oral administration of a single 10 mg/kg dose. This provided the plasma  $AUC_{0-6h}$  and the brain/plasma ratio (B/P) at 6 h, a measure of CNS penetrability.

Compounds **36**, **65** and **67**, from the coumarin, isocoumarin and pyridopyrimidinone series respectively, showed excellent in vitro activity, but all had moderate-to-poor brain and/or plasma exposure when administered orally to rats (Table 9). We determined that judicious placement of small alkyl groups resulted in a minor reduction in activity but improved both plasma and brain exposure. The observed improvements did not seem to be related to permeability or efflux, since these properties were largely unaffected by the additional alkyl groups as determined by measuring bidirectional membrane permeability across a Caco-2 cell monolayer. In general, the compounds exhibited modest permeability with minimal efflux. In the coumarin series, administration of the *N*-methyl analog **75** resulted in undetectable plasma concentrations. When  $R_1$  and  $R_2$  were both methyl (**49**), the 2-fold reduction in activity vs. **36** was compensated for by a significant improvement in plasma exposure, with a brain/plasma ratio of 0.7. The addition of

another methyl group at R<sub>3</sub> (**76**) resulted in a 2-fold decrease in activity compared to that of **49**, but greatly increased the brain/plasma ratio (B/P). Replacing the methyl group at R<sub>1</sub> in **76** with ethyl (**9**) achieved improvements in activity and plasma exposure. In the isocoumarin series methylation at R<sub>1</sub> and R<sub>2</sub> (**14**) was sufficient to improve plasma exposure and achieve a B/P ratio of 11. Similarly, in the pyridopyrimidinone series, methylation at R<sub>1</sub> and R<sub>2</sub> (**20**) resulted in improved exposure. Pyridopyrimidinone **20** had comparable brain and plasma exposures (B/P = 1.6), suggesting a more favorable distribution than observed for coumarin **9** (B/P = 19) and isocoumarin **14** (B/P = 11). Additionally, pyridopyrimidinone **20** has the advantage of lower plasma protein binding (80%) compared to that of coumarin **9** (96%) and isocoumarin **14** (93%).

**Table 9.** Effect of small alkyl group substitution on activity and pharmacokinetics

Compd	R <sub>1</sub>	R <sub>2</sub>	R <sub>3</sub>	EC <sub>1.5X PRO</sub> (nM)	Caco-2		PPB <sub>H</sub> (% bound)	Rat PK <sup>a</sup> (10 mg/kg, PO)	
					P <sub>app</sub> <sup>6</sup> (x 10 <sup>-6</sup> cm/s)	B-A / A-B		AUC <sub>0-6h</sub> (μg·h/mL)	B/P (6 h)
<b>36</b>	H	Me	H	15	—	—	—	0.34	6.5
<b>75</b>	Me	H	H	69	2.7	0.74	97	<0.01	n.d. <sup>b</sup>
<b>49</b>	Me	Me	H	31	1.4	1.1	97	0.53	0.7
<b>76</b>	Me	Me	(S)-Me	63	—	—	—	0.26	19
<b>9</b>	Et	Me	(S)-Me	44	1.2	1.9	96	1.1	19
<b>65</b>	H	Me	—	39	4.4	2.6	90	0.28	0.6
<b>77</b>	Me	H	—	120	—	—	—	<0.01	n.d. <sup>b</sup>
<b>14</b>	Me	Me	—	120	1.2	1.3	93	0.79	11

	<b>67</b>	H	Me	—	31	14	2.8	70	0.38	<0.1
	<b>78</b>	Me	H	—	300	—	—	—	<0.01	n.d. <sup>b</sup>
	<b>20</b>	Me	Me	—	160	7.5	1.7	80	2.1	1.6

<sup>a</sup> Dosed PO as a suspension at 10 mg/kg in 0.5% hydroxypropyl methylcellulose and 0.1% Tween-80 to male Sprague-Dawley rats.

<sup>b</sup> Not determined due to low compound concentration in the plasma.

### Pharmacodynamic response. Coumarin **9**, isocoumarin **14** and pyridopyrimidinone **20**

demonstrated oral and CNS exposure in rats sufficient to warrant further evaluation in the  $\Delta 7$  mouse model of SMA. The  $\Delta 7$  transgenic mouse produces low levels of human SMN protein and exhibits a severe SMA disease phenotype.<sup>29</sup> The median survival time (MST) of untreated  $\Delta 7$  mice is <20 days. Based on the in vitro data, we anticipated that our compounds would increase the level of SMN protein in  $\Delta 7$  mouse tissues by modifying *SMN2* alternative splicing, leading to a survival benefit when compared to untreated mice. The early manifestation of disease in  $\Delta 7$  mice necessitates the administration of compound at the neonatal developmental stage. We found that intraperitoneal dosing (IP) to neonates produced more consistent results than oral dosing. Prior to dosing  $\Delta 7$  mice, we determined plasma and brain exposure levels of **9**, **14** and **20** after a single 10 mg/kg IP dose to neonatal mice administered on postnatal day 9 (PND9) (Table 10). Each compound showed sufficient plasma and brain exposure ( $AUC_{0-24h}$ ) to conduct the pharmacodynamic and survival studies in  $\Delta 7$  mice. The compounds were administered as a DMSO solution once daily (QD) by IP injection. After 7 days of dosing, brain, spinal cord and quadriceps muscle were collected. All three compounds at a dose as low as 0.1 mg/kg demonstrated a dose dependent increase of SMN protein in all tissues analyzed (Table 10).

**Table 10:** Pharmacokinetic and pharmacodynamic data for **9**, **14** and **20**

Compd	EC <sub>1.5X PRO</sub> (nM)	Neonatal mouse PK IP, 10 mg/kg <sup>a</sup>			Δ7 mouse PD, IP, QD (PND3-PND9) <sup>a</sup>		
		AUC <sub>0-24h</sub> (μg·h/mL)	B/P	Dose mg/kg (N) <sup>b</sup>	SMN % increase above vehicle <sup>c</sup>		
					brain	spinal cord	quad
<b>9</b>	44	3.6	18	0.03 (7)	-10±11	7±20	-3±29
				0.1 (6)	115±49**	92±34**	154±70***
				0.3 (6)	194±37***	164±27***	147±36***
<b>14</b>	120	5.0	17	0.1 (7)	66±28**	35±18*	14±38
				0.3 (5)	114±49**	98±49***	83±83
				1 (10)	345±63***	203±48***	343±101***
				3 (11)	395±31***	284±96***	517±218***
<b>20</b>	160	6.9	2.9	0.1 (6)	43±32	26±19	6±16
				0.3 (7)	61±23*	67±22***	33±18
				1 (7)	149±57***	123±23***	129±33***
				3 (7)	230±65***	189±30***	218±75***

Abbreviations: B/P = brain to plasma ratio; PND = postnatal day; quad = quadriceps; IP = intraperitoneal; and QD = once daily.

<sup>a</sup> Dosed IP as a solution in 100% DMSO (2.5 mL/kg).

<sup>b</sup> Number of mice per dose group

<sup>c</sup> SMN % increase ± SD

\* p<0.05, \*\*p<0.01, \*\*\*p<0.001

To determine if the administration of compounds **9**, **14** and **20** to Δ7 mice would produce a survival benefit (an increase in median survival time), we chose doses that would elicit at least 100% increase in SMN protein in the brain. Coumarin **9**, isocoumarin **14**, and pyridopyrimidinone **20** were dosed IP as low as 0.1, 0.1, and 1 mg/kg daily, respectively. We switched to oral dosing twice a day at PND24 and increased the daily dose 6-fold above the IP dose to maintain the same drug levels in the plasma and tissue throughout the course of the study. All three compounds dose-dependently improved survival with higher doses resulting in long-term survival (Table 11).<sup>30-32</sup> Overall, our data show that treatment of Δ7 mice with compounds from multiple chemotypes (**9**, **14**, and **20**) results in increased SMN protein production in the CNS and peripheral tissues in a dose dependent manner and that these increases in SMN protein correlate with improved survival outcome.

**Table 11:**  $\Delta 7$  mouse survival data for **9**, **14** and **20**

Compd	IP dose <sup>a</sup> mg/kg/day (PND3-23)	PO dose <sup>b</sup> mg/kg/day (PND24→)	MST (d)	Survival at study conclusion <sup>c</sup> (PND concluded)
<b>Vehicle</b>	—	—	14	0/12 (21)
<b>9</b>	0.1	0.6	34	2/12 (55)
<b>9</b>	0.3	2	>55	8/14 (55)
<b>9</b>	1	6	>150	8/15 (150)
<b>14</b>	0.1	0.6	>100	7/11 (100)
<b>14</b>	0.3	2	>100	7/12 (100)
<b>20</b>	1	6	45	7/15 (90)
<b>20</b>	3	20	>190	7/11 (190)

Abbreviations: PND = postnatal day, MST = median survival time

<sup>a</sup> Dosed as a solution in DMSO (2.5 mL/kg).

<sup>b</sup> Dosed as a suspension in 0.5% hydroxypropyl methylcellulose and 0.1% Tween-80.

<sup>c</sup> Number of mice surviving/number of mice enrolled

## CONCLUSION

Through the discovery and activity-based optimization of 7-piperazinyl coumarins, we have identified three novel classes of molecules that potently shift splicing of *SMN2* pre-mRNA to favor the production of *SMN2-FL* mRNA over *SMN2- $\Delta 7$*  mRNA. This shift causes cells that are deficient in SMN protein (due to the lack of the *SMN1* gene) to produce additional and fully functional SMN protein, which is critical for the proper function of cells, particularly motor neurons. Compounds that exhibited potent in vitro activity in SMA patient-derived fibroblasts were further optimized for oral delivery to disease relevant tissues in rats and mice. We demonstrated that the levels of SMN protein could be increased in a dose dependent manner in brain, spinal cord and muscle tissue in  $\Delta 7$  mice after the administration of compounds derived

1  
2  
3 from all three classes of molecules. Daily administration of these compounds to  $\Delta 7$  mice resulted  
4  
5 in a reduction of disease manifestations and a significant increase in median survival time. These  
6  
7 findings support the development of orally administered small molecules for the treatment of  
8  
9 patients with SMA.  
10  
11

## 12 13 14 **EXPERIMENTAL METHODS**

15  
16  
17 Starting materials and other reagents were purchased from commercial suppliers and were used  
18  
19 without further purification unless otherwise indicated. The syntheses of intermediates utilized  
20  
21 here (**1b** and **1c**) are described in the Supporting Information. Air or moisture sensitive reactions  
22  
23 were performed under either a nitrogen or argon atmosphere. Flash chromatography was  
24  
25 performed using silica gel with standard techniques or with silica gel cartridges on an ISCO  
26  
27 Combiflash chromatography instrument.  $^1\text{H}$  NMR spectra were recorded at 500 MHz on a  
28  
29 Bruker NMR spectrometer. The chemical shifts are given in ppm referenced to the deuterated  
30  
31 solvent signal. Coupling constants ( $J$ ) are recorded in hertz. LC-MS analyses were performed on  
32  
33 a Waters Acquity UPLC/MS system with an analytical C18 column and compounds were  
34  
35 detected by UV absorption at 254 nm. All final compounds with reported biological data were  
36  
37 determined to be >95% pure as determined by LC/MS and  $^1\text{H}$  NMR unless otherwise noted.  
38  
39  
40  
41  
42

43  
44 **Ethyl 2-(benzo[d]oxazol-2-yl)acetate (1a).** A mixture of 2-aminophenol (5.0 g, 46 mmol) and  
45  
46 ethyl 3-ethoxy-3-iminopropanoate hydrochloride (11.7 g, 60 mmol) in EtOH (200 mL) was  
47  
48 stirred at 80 °C for 16 h. The mixture was partitioned between EtOAc (200 mL) and H<sub>2</sub>O (200  
49  
50 mL). The organic layer was washed with brine and concentrated. The residue was  
51  
52 chromatographed on silica gel (10% EtOAc in hexanes) to yield **1a** (9.0 g, 95%) as a pale yellow  
53  
54  
55  
56  
57  
58  
59  
60

oil.  $^1\text{H}$  NMR (DMSO- $d_6$ )  $\delta$  7.74 (m, 2H), 7.44-7.37 (m, 2H), 4.22 (s, 2H), 4.17 (q,  $J = 7.1$  Hz, 2H), 1.22 (t,  $J = 7.1$  Hz, 3H).

**tert-Butyl 4-(4-formyl-3-hydroxyphenyl)piperazine-1-carboxylate (2).** A mixture of 4-fluorosalicylaldehyde (2.80 g, 20 mmol) and 1-Boc-piperazine (4.47 g, 24 mmol) in DMSO (20 mL) was heated at 100 °C for 16 h. The mixture was diluted with H<sub>2</sub>O (100 mL) and extracted with EtOAc (100 mL). The organic layer was washed with brine, dried over Na<sub>2</sub>SO<sub>4</sub>, filtered and concentrated. The residue was chromatographed on silica gel (0-50% EtOAc in hexanes) to yield **2** (4.6 g, 75%) as a tan solid. LC-MS:  $m/z = 307.2$  [M+H]<sup>+</sup>.  $^1\text{H}$  NMR (500 MHz, CDCl<sub>3</sub>)  $\delta$  11.39 (br s, 1H), 9.55 (s, 1H), 7.31 (d,  $J = 8.8$  Hz, 1 H), 6.47 (dd,  $J = 8.8, 2.5$  Hz, 1H), 6.26 (d,  $J = 2.2$  Hz, 1H), 3.55 (m, 4H), 3.35 (m, 4H), 1.42 (s, 9H).

**tert-Butyl 4-(3-(benzo[d]oxazol-2-yl)-2-oxo-2H-chromen-7-yl)piperazine-1-carboxylate (3).** Compound **1a** (100 mg, 0.43 mmol), compound **2** (138 mg, 0.45 mmol), AcOH (15  $\mu\text{L}$ , 0.25 mmol) and piperidine (44  $\mu\text{L}$ , 0.45 mmol) were combined in EtOH (2 mL). The mixture was stirred in a sealed tube at 90 °C for 24 h. After cooling to rt, the mixture was filtered. The solid was washed with Et<sub>2</sub>O and dried, yielding **3** (180 mg, 93%). LC-MS:  $m/z = 448.2$  [M+H]<sup>+</sup>.

**3-(Benzo[d]oxazol-2-yl)-7-(piperazin-1-yl)-2H-chromen-2-one hydrochloride (4).** Compound **3** (90 mg, 0.2 mmol) was dissolved in 4 N HCl in 1,4-dioxane (2 mL). The mixture was stirred at rt for 3 h. The solid was collected and dried, yielding **4** (66 mg, 85%) as a yellow powder. LC-MS:  $m/z = 348.2$  [M+H]<sup>+</sup>.  $^1\text{H}$  NMR (500 MHz, CDCl<sub>3</sub>)  $\delta$  9.31 (br s, 2H), 8.92 (s, 1H), 7.84-7.76 (3H), 7.44 (m, 2H), 7.12 (dd,  $J = 9.0, 2.2$  Hz, 1H), 7.01 (d,  $J = 2.2$  Hz, 1H), 3.75 (m, 4H), 3.23 (m, 4H).

1  
2  
3 **3-Acetyl-7-fluoro-2H-chromen-2-one (5)**. Piperidine (100  $\mu$ L, 1 mmol) was added to a mixture  
4  
5 of 4-fluoro-2-hydroxybenzaldehyde (1.4 g, 10 mmol) and ethyl 3-oxobutanoate (1.3 g, 10  
6  
7 mmol). The mixture was stirred at rt for 10 min. The precipitate that formed was collected by  
8  
9 vacuum filtration. The solid was washed with ethanol and aqueous HCl (1 N), filtered and dried  
10  
11 to give **5** (1.96 g, 95%) as a pale yellow solid.  $^1\text{H}$  NMR (500 MHz,  $\text{CDCl}_3$ )  $\delta$  8.51 (s, 1H), 7.68  
12  
13 (m, 1H), 7.13-7.07 (m, 2H), 2.73 (s, 3H).  
14  
15  
16  
17

18 **3-(2-Bromoacetyl)-7-fluoro-2H-chromen-2-one (6)**. A solution of bromine (1.6 g, 10 mmol) in  
19  
20  $\text{CHCl}_3$  (10 mL) was added dropwise to a solution of **5** (1.96 g, 9.5 mmol) in  $\text{CHCl}_3$  (20 mL). The  
21  
22 mixture was stirred at rt for 1 h. The solid material that was present in the mixture was collected  
23  
24 by vacuum filtration, washed with  $\text{CHCl}_3$  and dried to give **6** (1.96 g, 72%) as a pale yellow  
25  
26 solid.  $^1\text{H}$  NMR (500 MHz,  $\text{CDCl}_3$ )  $\delta$  8.63 (s, 1H), 7.72 (m, 1H), 7.17-7.10 (m, 2H), 4.73 (s, 2H).  
27  
28  
29  
30

31 **3-(6,8-Dimethylimidazo[1,2-a]pyrazin-2-yl)-7-fluoro-2H-chromen-2-one hydrobromide (7)**.  
32  
33 A mixture of **6** (0.684 g, 2.4 mmol) and 3,5-dimethylpyrazin-2-amine (0.246 g, 2.0 mmol) in  
34  
35  $\text{CH}_3\text{CN}$  (10 mL) was stirred at 120  $^\circ\text{C}$  in a sealed tube for 20 min. The mixture was cooled to rt  
36  
37 and diluted with  $\text{Et}_2\text{O}$  to produce a precipitate. The solid was collected by vacuum filtration,  
38  
39 washed with  $\text{Et}_2\text{O}$  and dried to give **7** (0.7 g, 90%) as a tan solid. LC-MS:  $m/z = 310.1$   $[\text{M}+\text{H}]^+$ .  
40  
41  $^1\text{H}$  NMR (500 MHz,  $\text{DMSO}-d_6$ )  $\delta$  8.92 (s, 1H), 8.84 (s, 1H), 8.58 (s, 1H), 8.10 (dd,  $J = 6.3, 8.8$   
42  
43 Hz, 1H), 7.48 (dd,  $J = 2.3, 9.6$  Hz, 1H), 7.33 (dt,  $J = 2.5, 8.7$  Hz, 1H), 2.91 (s, 3H), 2.46 (s, 3H).  
44  
45  
46  
47  
48

49 **(S)-3-(6,8-Dimethylimidazo[1,2-a]pyrazin-2-yl)-7-(3-methylpiperazin-1-yl)-2H-chromen-2-**  
50  
51 **one (8)**. Compound **7** (100 mg, 0.25 mmol) was combined with (*S*)-2-methylpiperazine (52 mg,  
52  
53 0.52 mmol) and  $\text{K}_2\text{CO}_3$  (0.14 g, 1.0 mmol) in DMSO (0.5 mL). The mixture was stirred at 120  
54  
55  $^\circ\text{C}$  for 2 h. The mixture was cooled to rt and diluted with water to produce a precipitate. The  
56  
57  
58  
59  
60

1  
2  
3 solid was collected by vacuum filtration and purified by silica gel chromatography (10 % MeOH  
4 in CH<sub>2</sub>Cl<sub>2</sub>) to give **8** (64 mg, 64%) as a yellow solid. LC–MS:  $m/z = 390.2$  [M+H]<sup>+</sup>. <sup>1</sup>H NMR  
5 (500 MHz, CDCl<sub>3</sub>): δ 8.74 (s, 1H), 8.45 (s, 1H), 7.77 (s, 1H), 7.51 (d,  $J = 8.8$  Hz, 1H), 6.88 (dd,  
6  $J = 8.8$  Hz, 2.5 Hz, 1H), 6.77 (d,  $J = 2.5$  Hz, 1H), 3.77-3.67 (m, 2H), 3.21-3.14 (m, 2H), 3.06-  
7 2.92 (m, 3H), 2.91 (s, 3H), 2.64-2.56 (m, 1H), 2.48 (s, 3H), 1.20 (d,  $J = 6.3$  Hz, 3H).  
8  
9  
10  
11  
12  
13  
14  
15

16 **(S)-3-(6,8-Dimethylimidazo[1,2-a]pyrazin-2-yl)-7-(4-ethyl-3-methylpiperazin-1-yl)-2H-**  
17 **chromen-2-one (9)**. A mixture of **8** (250 mg, 0.64 mmol), acetaldehyde (71 μL, 1.29 mmol) and  
18 sodium triacetoxyborohydride (409 mg, 1.93 mmol) in 10% MeOH in CH<sub>2</sub>Cl<sub>2</sub> (10 mL) was  
19 stirred at rt overnight. The excess reagent was quenched by the addition of aqueous saturated  
20 NaHCO<sub>3</sub>. The mixture was extracted with CH<sub>2</sub>Cl<sub>2</sub> (10% MeOH). The organic layer was dried  
21 over NaSO<sub>4</sub>, filtered, concentrated and purified by silica gel column chromatography (10%  
22 MeOH in CH<sub>2</sub>Cl<sub>2</sub>) to give **9** (192 mg, 72%) as a yellow solid: mp 208–209 °C. LC–MS:  $m/z =$   
23 418.1 [M+H]<sup>+</sup>. <sup>1</sup>H NMR (500 MHz, DMSO-*d*<sub>6</sub>) δ 8.70 (s, 1H), 8.50 (s, 1H), 8.30 (d,  $J = 0.9$  Hz,  
24 1H), 7.73 (d,  $J = 8.8$  Hz, 1H), 7.02 (s, 1H), 6.88 (d,  $J = 1.9$  Hz, 1H), 3.73 (br s, 2H), 3.04 (m,  
25 1H), 2.86 (m, 1H), 2.81-2.71 (5H), 2.44 (m, 1H), 2.38-2.26 (5H), 1.06 (d,  $J = 6.3$  Hz, 3H), 0.98  
26 (t,  $J = 7.0$  Hz, 3H).  
27  
28  
29  
30  
31  
32  
33  
34  
35  
36  
37  
38  
39  
40  
41  
42

43 **7-Fluoro-3-(1-hydroxyethyl)-1H-isochromen-1-one (10)**. A mixture of 5-fluoro-2-iodobenzoic  
44 acid (9.04 g, 34.0 mmol), but-3-yn-2-ol (5.7 mL, 5.46 g, 78.0 mmol), ZnCl<sub>2</sub> (4.62 g, 34.0 mmol),  
45 Pd(PPh<sub>3</sub>)<sub>4</sub> (1.96 g, 1.7 mmol), Et<sub>3</sub>N (14.2 mL, 10.3 g, 102.0 mmol) and DMF (50 mL) was  
46 stirred under argon at 100 °C for 2 h. After the removal of the volatiles under vacuum, the  
47 residue was chromatographed on silica gel (0-50% ethyl acetate in hexanes) to provide **10** (5.93  
48 g, 84%) as a brown oil. LC–MS:  $m/z = 209.2$  [M+H]<sup>+</sup>. <sup>1</sup>H NMR (500 MHz, CDCl<sub>3</sub>): δ 7.94 (m,  
49 1H), 7.47-7.43 (2H), 6.57 (m, 1H), 4.67 (q,  $J = 6.5$  Hz, 1H), 1.57 (d,  $J = 6.6$  Hz, 3H).  
50  
51  
52  
53  
54  
55  
56  
57  
58  
59  
60

1  
2  
3 **3-Acetyl-7-fluoro-1H-isochromen-1-one (11)**. To a solution of compound **10** (5.93 g, 28.5  
4 mmol) in CH<sub>2</sub>Cl<sub>2</sub> (50 mL) was added MnO<sub>2</sub> (24.8 g, 285 mmol). The mixture was stirred  
5 vigorously at rt for 48 h and then the volatiles were removed by rotary evaporation. The resulting  
6 residue was suspended in CH<sub>2</sub>Cl<sub>2</sub> (500 mL), stirred for 0.5 h, and then filtered. The solid was  
7 washed with additional CH<sub>2</sub>Cl<sub>2</sub> (4 x 100 mL). The combined filtrates were concentrated and  
8 chromatographed on silica gel (0-20% EtOAc in CH<sub>2</sub>Cl<sub>2</sub>) to provide **11** (3.88 g, 66%) as white  
9 needles. LC-MS: *m/z* = 207.1 [M+H]<sup>+</sup>. <sup>1</sup>H NMR (500 MHz, CDCl<sub>3</sub>) δ 8.03 (m, 1H), 7.68 (dd, *J*  
10 = 8.5, 5.0 Hz, 1H), 7.54 (m, 1H), 7.40 (d, *J* = 0.6 Hz, 1H), 2.59 (s, 3H).  
11  
12  
13  
14  
15  
16  
17  
18  
19  
20  
21  
22

23 **3-(2-Bromoacetyl)-7-fluoro-1H-isochromen-1-one (12)**. To a solution of **11** (2.63 g, 12.8  
24 mmol) in CHCl<sub>3</sub> (30 mL) was added bromine (0.72 mL, 14.0 mmol). The mixture was stirred at  
25 rt for 1 h. Hexanes (150 mL) were added to the mixture. After stirring for 15 min, the precipitate  
26 was collected by filtration. The solid was washed with hexanes and water, and then dried.  
27  
28 Separately, the CHCl<sub>3</sub> filtrate was washed with aqueous saturated NaHCO<sub>3</sub>. The organic layer  
29 was concentrated. The residue was then chromatographed on silica gel (0-5% EtOAc in CH<sub>2</sub>Cl<sub>2</sub>).  
30 The chromatographed material was combined with the solid material collected by precipitation to  
31 yield **12** (3.48 g, 96%). LC-MS: *m/z* = 283.0, 285.0 [M-H]<sup>-</sup>. <sup>1</sup>H NMR (500 MHz, CDCl<sub>3</sub>): δ 8.05  
32 (dd, *J* = 8.2, 2.8 Hz, 1H), 7.72 (dd, *J* = 8.5, 5.0 Hz, 1H), 7.57 (m, 1H), 7.52 (s, 1H), 4.47 (s, 2H).  
33  
34  
35  
36  
37  
38  
39  
40  
41  
42  
43  
44

45 **3-(6,8-Dimethylimidazo[1,2-a]pyrazin-2-yl)-7-fluoro-1H-isochromen-1-one hydrobromide**  
46 **(13)**. Compound **12** (1.43 g, 5.0 mmol) was combined with 3,5-dimethylpyrazin-2-amine (0.67 g,  
47 5.5 mmol) and CH<sub>3</sub>CN (10 mL) in a sealed tube. The mixture was stirred at 100 °C overnight.  
48 After cooling the mixture to rt, EtOAc (20 mL) was added. The precipitate that formed was  
49 collected, washed with EtOAc and dried, providing **13** (1.81 g, 93%). LC-MS: *m/z* = 310.3  
50 [M+H]<sup>+</sup>; <sup>1</sup>H NMR (500 MHz, DMSO-*d*<sub>6</sub>) δ 8.00 (d, *J* = 1.6 Hz, 1H), 7.91 (d, *J* = 0.6 Hz, 1H),  
51  
52  
53  
54  
55  
56  
57  
58  
59  
60

1  
2  
3 7.78 (dd,  $J = 8.8, 2.8$  Hz, 1H), 7.73-7.63 (m, 2H), 7.27 (s, 1H), 7.14 (t,  $J = 1.3$  Hz, 1H), 2.55 (s,  
4 3H), 2.26 (d,  $J = 0.9$  Hz, 3H).  
5  
6  
7

8  
9 **3-(6,8-Dimethylimidazo[1,2-a]pyrazin-2-yl)-7-(4-methylpiperazin-1-yl)-1H-isochromen-1-**  
10 **one (14).** Compound **13** (390 mg, 1.0 mmol), N-methylpiperazine (300 mg, 3.0 mmol) and NMP  
11 (2.0 mL) were combined and stirred at 180 °C for 24 h under argon. After cooling to rt, the  
12 mixture was chromatographed on silica gel (0-30% MeOH in CH<sub>2</sub>Cl<sub>2</sub>) to provide **14** (223 mg,  
13 57%) as a yellow powder: mp 240-241 °C. LC-MS:  $m/z = 390.1$  [M+H]<sup>+</sup>. <sup>1</sup>H NMR (500 MHz,  
14 DMSO-*d*<sub>6</sub>) δ 8.34 (s, 1H), 8.26 (m, 1H), 7.70 (d,  $J = 8.8$  Hz, 1H), 7.57 (dd,  $J = 8.8, 2.5$  Hz, 1H),  
15 7.50 (d,  $J = 2.5$  Hz, 1H), 7.42 (s, 1H), 3.31-3.26 (m, 4H), 2.74 (s, 3H), 2.49-2.45 (m, 4H), 2.38  
16 (d,  $J = 1.0$  Hz, 3H), 2.24 (s, 3H).  
17  
18  
19  
20  
21  
22  
23  
24  
25  
26  
27

28  
29 **Ethyl 4-hydroxy-6-methylpyrazolo[1,5-a]pyrazine-2-carboxylate (15).** To a solution of  
30 diethyl 1H-pyrazole-3,5-dicarboxylate (10.0 g, 47 mmol) and chloroacetone (3.76 mL, 47 mmol)  
31 in acetone (200 mL) was added potassium carbonate (7.2 g, 52 mmol). After heating at 30 °C for  
32 6 h, the mixture was concentrated. The residue was partitioned between EtOAc and water. The  
33 organic layer was collected and dried over MgSO<sub>4</sub>. The mixture was filtered and concentrated to  
34 give a light brown solid MS  $m/z = 269.1$  [M+H]<sup>+</sup>, which was used directly in the next step. To the  
35 residue was added AcOH (300 mL) and ammonium acetate (72 g, 940 mmol). After refluxing for  
36 48 h, the mixture was concentrated and then diluted with water to form a precipitate. The solid  
37 was collected by filtration, washed sequentially with water and CH<sub>3</sub>CN, and then dried to give  
38 **15** (6.7 g, 64%) as a tan solid. LC-MS:  $m/z = 222.1$  [M+H]<sup>+</sup>. <sup>1</sup>H NMR (500 MHz, DMSO-*d*<sub>6</sub>) δ  
39 11.25 (br s, 1H), 7.63 (s, 1H), 7.33 (s, 1H), 4.33 (q,  $J = 7.0$  Hz, 2H), 2.15 (s, 3H), 1.32 (t,  $J = 7.0$   
40 Hz, 3H).  
41  
42  
43  
44  
45  
46  
47  
48  
49  
50  
51  
52  
53  
54  
55  
56  
57  
58  
59  
60

1  
2  
3 **Ethyl 4-chloro-6-methylpyrazolo[1,5-a]pyrazine-2-carboxylate (16).** A mixture of **15** (7.18 g,  
4 32.5 mmol) and POCl<sub>3</sub> (80 mL) was stirred at reflux for 15 h. The dark mixture was concentrated  
5 and suspended in CH<sub>3</sub>CN. The solid material was collected to give **16** (5.20 g) as an off-white  
6 solid. The filtrate was concentrated and chromatographed on silica gel (0-10% EtOAc in CH<sub>2</sub>Cl<sub>2</sub>)  
7 to give an additional 1.42 g of product (total of 6.62 g, 85%). LC-MS: *m/z* = 240.1, 242.1  
8 [M+H]<sup>+</sup>. <sup>1</sup>H NMR (500 MHz, DMSO-*d*<sub>6</sub>) δ 8.82 (m, 1H), 7.41 (d, *J* = 1.3 Hz, 1H), 4.38 (q, *J* =  
9 7.0 Hz, 2 H), 2.45 (m, 3H), 1.34 (t, *J* = 7.1 Hz, 3H).  
10  
11  
12  
13  
14  
15  
16  
17  
18  
19

20  
21 **Ethyl 4,6-dimethylpyrazolo[1,5-a]pyrazine-2-carboxylate (17).** A mixture of compound **16**  
22 (5.20 g, 21.7 mmol), methylboronic acid (3.90 g, 65.1 mmol), K<sub>2</sub>CO<sub>3</sub> (14.8 g, 107.5 mmol) and  
23 Pd(PPh<sub>3</sub>)<sub>2</sub>Cl<sub>2</sub> (456 mg, 0.65 mmol) and DMF (100 mL) was degassed and heated at 100 °C  
24 under N<sub>2</sub> for 15 h. The mixture was concentrated by rotary evaporation. The residue was  
25 chromatographed on silica gel (2-5% MeOH in CH<sub>2</sub>Cl<sub>2</sub>) to give **17** (3.90 g, 82%) as a yellow  
26 solid. LC-MS: *m/z* = 220.1 [M+H]<sup>+</sup>. <sup>1</sup>H NMR (500 MHz, DMSO-*d*<sub>6</sub>) δ 8.54 (s, 1H), 7.49 (s, 1H),  
27 4.36 (q, *J* = 7.2 Hz, 2H), 2.70 (s, 3H), 2.42 (s, 3H), 1.34 (t, *J* = 7.2 Hz, 3H).  
28  
29  
30  
31  
32  
33  
34  
35  
36  
37

38 **Ethyl 3-(4,6-dimethylpyrazolo[1,5-a]pyrazin-2-yl)-3-oxopropanoate (18).** To a solution of *t*-  
39 butyl acetate (4.80 mL, 35.6 mmol) in THF (200 mL) at -78 °C was added LDA (2.0 M, 21.4  
40 mL, 42.7 mmol). After 0.5 h, the solution was cannulated into a solution of **17** (3.90 g, 17.8  
41 mmol) in THF (100 mL) at -30 °C. After 1 h, the excess reagent was quenched with saturated  
42 aqueous NH<sub>4</sub>Cl. The mixture was then partitioned in EtOAc and H<sub>2</sub>O (adjusted to pH 5-6). The  
43 organic layer was dried over MgSO<sub>4</sub>, filtered and concentrated. The residue was  
44 chromatographed on silica gel (2-4% MeOH in CH<sub>2</sub>Cl<sub>2</sub>) to give 5.01 g (97%) of tert-butyl ester  
45 intermediate as a yellow oil, which solidified upon standing. LC-MS: *m/z* = 290.2 [M+H]<sup>+</sup>; <sup>1</sup>H  
46 NMR (500 MHz, DMSO-*d*<sub>6</sub>): δ 8.57 (s, 1H), 7.50 (s, 1H), 4.02 (s, 2H), 2.70 (s, 3H), 2.43 (s, 3H),  
47  
48  
49  
50  
51  
52  
53  
54  
55  
56  
57  
58  
59  
60

1  
2  
3 1.38 (s, 9H). The intermediate (4.86 g, 16.8 mmol) was heated at 120 °C in EtOH (30 mL) in a  
4 capped tube. After 1 h, the solution was cooled to rt and the volatiles were removed to give **18**  
5  
6 (4.44 g, 98%) as a yellow solid. LC–MS:  $m/z = 262.2$   $[M+H]^+$ .  $^1\text{H}$  NMR (500 MHz, acetone- $d_6$ )  
7  
8  $\delta$  8.37 (dd,  $J = 1.9, 0.9$  Hz, 1H), 7.38 (d,  $J = 0.9$  Hz, 1H), 4.17 (q,  $J = 7.3$  Hz, 2H), 4.12 (s, 2H),  
9  
10 2.76 (d,  $J = 0.6$  Hz, 3H), 2.49 (d,  $J = 0.9$  Hz, 3H), 1.23 (m, 3H).  
11  
12  
13  
14  
15

16 **2-(4,6-Dimethylpyrazolo[1,5-a]pyrazin-2-yl)-7-fluoro-4H-pyrido[1,2-a]pyrimidin-4-one**

17  
18 **(19)**. A mixture of 2-amino-5-fluoro-pyridine (134 mg, 1.2 mmol), compound **18** (261 mg, 1.0  
19 mmol) and pyridinium *p*-toluenesulfonate (12.6 mg, 0.05 mmol) was heated at 130 °C. After 8 h,  
20  
21 the mixture was cooled to rt and chromatographed on silica gel (2-4% MeOH in  $\text{CH}_2\text{Cl}_2$ ) to give  
22  
23 **19** (220 mg, 71%) as a yellow solid. LC–MS:  $m/z = 310.2$   $[M+H]^+$ .  $^1\text{H}$  NMR (500 MHz, DMSO-  
24  
25  $d_6$ ):  $\delta$  8.96 (m, 1H), 8.55 (s, 1H), 8.14 (m, 1H), 7.86 (m, 1H), 7.56 (s, 1H), 7.03 (s, 1H), 2.73 (s,  
26  
27 3H), 2.43 (s, 3H).  
28  
29  
30  
31  
32  
33

34 **2-(4,6-Dimethylpyrazolo[1,5-a]pyrazin-2-yl)-7-(4-methylpiperazin-1-yl)-4H-pyrido[1,2-**

35  
36 **a]pyrimidin-4-one (20)**. Compound **19** (309 mg, 1.0 mmol) and *N*-methylpiperazine (1.1 mL,  
37 10 mmol) in DMA (1.0 mL) was stirred at 150 °C for 15 h. After cooling to rt and diluting with  
38  
39  $\text{CH}_3\text{CN}$  (5 mL), the mixture was filtered. The solid was washed with  $\text{CH}_3\text{CN}$  and dried to yield  
40  
41 **20** (313 mg, 80%) as a yellow solid: mp 254-256 °C. LC–MS:  $m/z = 390.4$   $[M+H]^+$ .  $^1\text{H}$  NMR  
42  
43 (500 MHz, DMSO- $d_6$ )  $\delta$  8.55 (s, 1H), 8.27 (d,  $J = 2.7$  Hz, 1H), 8.12 (dd,  $J = 9.7, 2.8$  Hz, 1H),  
44  
45 7.71 (d,  $J = 9.7$  Hz, 1H), 7.54 (s, 1H), 6.95 (s, 1H), 3.25 (m, 4H), 2.72 (s, 3H), 2.51 (m, 4H), 2.43  
46  
47 (s, 3H), 2.25 (s, 3H).  
48  
49  
50  
51  
52  
53

54 **3-(Benzo[d]oxazol-2-yl)-7-(diethylamino)-2H-chromen-2-one (21)**. Compound **21** was

55 prepared from **1a** and 4-(diethylamino)-2-hydroxybenzaldehyde by following the procedure used  
56  
57  
58  
59  
60

1  
2  
3 to prepare **3**. LC–MS:  $m/z = 335.7$   $[M + H]^+$ .  $^1\text{H}$  NMR (500 MHz,  $\text{DMSO-}d_6$ )  $\delta$  8.81 (s, 1H),  
4  
5 7.75 (m, 2H), 7.71 (d,  $J = 9.0$  Hz, 1H), 7.40 (m, 2H), 6.83 (dd,  $J = 9.1, 2.5$  Hz, 1H), 6.62 (d,  $J =$   
6  
7 2.3 Hz, 1H), 3.48 (q,  $J = 7.2$  Hz, 4H), 1.27 (t,  $J = 7.1$  Hz, 6H).  
8  
9

10  
11 **3-(Benzo[d]oxazol-2-yl)-7-(dimethylamino)-2H-chromen-2-one (22)**. Compound **22** was  
12 prepared from **1a** and 4-(dimethylamino)-2-hydroxybenzaldehyde by following the procedure  
13 used to prepare **3**. LC–MS:  $m/z = 306.9$   $[M + H]^+$ .  $^1\text{H}$  NMR (500 MHz,  $\text{DMSO-}d_6$ )  $\delta$  8.85 (s,  
14  
15 1H), 7.79-7.72 (3H), 7.41 (m, 2H), 6.85 (dd,  $J = 8.8, 2.5$  Hz, 1H), 6.64 (d,  $J = 2.2$  Hz, 1H), 3.12  
16  
17 (s, 6H).  
18  
19  
20  
21  
22  
23

24 **3-(Benzo[d]oxazol-2-yl)-7-(piperidin-1-yl)-2H-chromen-2-one (23)**. Compound **23** was  
25 prepared from **1a** and 2-hydroxy-4-(piperidin-1-yl)benzaldehyde by following the procedure  
26 used to prepare **3**. LC–MS:  $m/z = 347.2$   $[M + H]^+$ .  $^1\text{H}$  NMR (500 MHz,  $\text{DMSO-}d_6$ )  $\delta$  8.82 (s,  
27  
28 1H), 7.76 (m, 2H), 7.71 (d,  $J = 9.0$  Hz, 1H), 7.40 (m, 2H), 7.04 (dd,  $J = 9.1, 2.2$  Hz, 1H), 6.85 (d,  
29  
30  $J = 1.9$  Hz, 1H), 3.52 (m, 4H), 1.64 (m, 2H), 1.59 (m, 4H).  
31  
32  
33  
34  
35  
36

37 **3-(Benzo[d]oxazol-2-yl)-7-morpholino-2H-chromen-2-one (24)**. Compound **24** was prepared  
38 from **1a** and 2-hydroxy-4-morpholinobenzaldehyde by following the procedure used to prepare  
39 **3**. LC–MS:  $m/z = 349.0$   $[M + H]^+$ .  $^1\text{H}$  NMR (500 MHz,  $\text{CDCl}_3$ )  $\delta$  8.59 (s, 1H), 7.76 (dd,  $J =$   
40  
41 6.15, 2.9 Hz, 1H), 7.53 (m, 1H), 7.43 (d,  $J = 8.8$  Hz, 1H), 7.29 (m, 2H), 6.79 (dd,  $J = 8.8, 2.5$  Hz,  
42  
43 1H), 6.67 (d,  $J = 2.2$  Hz, 1H), 3.81 (m, 4H), 3.32 (m, 4H).  
44  
45  
46  
47  
48  
49

50 **3-Phenyl-7-(piperazin-1-yl)-2H-chromen-2-one (25)**. Compound **25** was prepared from **2** and  
51 ethyl 2-phenylacetate by following the procedure used to prepare **4**. LC–MS:  $m/z = 307.0$   $[M +$   
52  
53  $\text{H}]^+$ .  $^1\text{H}$  NMR (500 MHz,  $\text{CDCl}_3$ )  $\delta$  7.97 (s, 1H), 7.70 (m, 2H), 7.55 (d,  $J = 8.8$  Hz, 1H), 7.43 (m,  
54  
55  
56  
57  
58  
59  
60

1  
2  
3 2H), 7.38 (m, 1H), 7.01 (dd,  $J = 8.8, 2.5$  Hz, 1H), 6.86 (d,  $J = 2.5$  Hz, 1H), 3.43 (m, 4H), 3.07  
4  
5 (m, 4H).  
6  
7

8  
9 **3-(4-Methoxyphenyl)-7-(piperazin-1-yl)-2H-chromen-2-one (26)**. Compound **26** was prepared  
10 from **2** and ethyl 2-(4-methoxyphenyl)acetate by following the procedure used to prepare **4**.  
11

12 LC-MS:  $m/z = 337.0$  [M + H]<sup>+</sup>. <sup>1</sup>H NMR (500 MHz, CDCl<sub>3</sub>)  $\delta$  8.05 (s, 1H), 7.70-7.65 (2H), 7.54  
13  
14 (d,  $J = 8.8$  Hz, 1H), 7.02-6.97 (3H), 6.83 (d,  $J = 2.2$  Hz, 1H) 3.80 (s, 3H), 3.30 (m, 4H), 2.86 (m,  
15  
16 4H).  
17  
18  
19

20  
21 **3-(3,4-Dimethoxyphenyl)-7-(piperazin-1-yl)-2H-chromen-2-one (27)**. Compound **27** was  
22 prepared from **2** and ethyl 2-(3,4-dimethoxyphenyl)acetate by following the procedure used to  
23  
24 prepare **4**. LC-MS:  $m/z = 367.2$  [M+H]<sup>+</sup>. <sup>1</sup>H NMR (500 MHz, CDCl<sub>3</sub>)  $\delta$  7.69 (s, 1H), 7.38 (d,  $J$   
25  
26 = 8.8 Hz, 1H), 7.31 (d,  $J = 1.9$  Hz, 1H), 7.25 (d,  $J = 2.2$  Hz, 1H), 6.93 (d,  $J = 8.5$  Hz, 1H), 6.85  
27  
28 (dd,  $J = 8.8$  Hz, 2.5 Hz, 1H), 6.77 (d,  $J = 2.5$  Hz, 1H), 3.95 (s, 3H), 3.93 (s, 3H), 3.36-3.32 (m,  
29  
30 4H), 3.10-3.05 (m, 4H).  
31  
32  
33  
34  
35  
36

37 **3-(Benzo[d]thiazol-2-yl)-7-(piperazin-1-yl)-2H-chromen-2-one hydrochloride (28)**.

38 Compound **28** was prepared from **2** and **1b** by following the procedure used to prepare **1**.  
39

40 LC-MS:  $m/z = 364.4$  [M+H]<sup>+</sup>. <sup>1</sup>H NMR (500 MHz, DMSO-*d*<sub>6</sub>)  $\delta$  9.26 (br s, 2H), 9.14 (s, 1H),  
41  
42 8.16 (d,  $J = 7.9$  Hz, 1H), 8.04 (d,  $J = 8.1$  Hz, 1H), 7.93 (d,  $J = 9.0$  Hz, 1H), 7.56 (m, 1H), 7.47  
43  
44 (m, 1H), 7.16 (dd,  $J = 8.9$  Hz, 2.3 Hz, 1H), 7.09 (d,  $J = 2.3$  Hz, 1H), 3.76-3.74 (m, 4H), 3.25-  
45  
46 3.23 (m, 4H).  
47  
48  
49  
50

51  
52 **3-(1H-benzo[d]imidazol-2-yl)-7-(piperazin-1-yl)-2H-chromen-2-one (29)**. Compound **29** was  
53 prepared from **2** and **1c** by following the procedure used to prepare **4**. LC-MS:  $m/z = 347.2$   
54

55 [M+H]<sup>+</sup>. <sup>1</sup>H NMR (500 MHz, DMSO-*d*<sub>6</sub>)  $\delta$  12.33 (s, 1H), 8.97 (s, 1H), 7.76 (d,  $J = 8.8$  Hz, 1H),  
56  
57  
58  
59  
60

1  
2  
3 7.66-7.60 (2H), 7.22-7.16 (2H), 7.07 (dd,  $J = 9.1, 2.2$  Hz, 1H), 6.92 (d,  $J = 2.2$  Hz, 1H), 3.38 (m,  
4  
5 4H), 2.83 (m, 4H).  
6  
7

8  
9 **3-(Imidazo[1,2-a]pyridin-2-yl)-7-(piperazin-1-yl)-2H-chromen-2-one (30).** Compound **30** was  
10 prepared from **6** and 2-aminopyridine by following the procedure used to prepare **8**. LC-MS:  $m/z$   
11 = 347.1 [M+H]<sup>+</sup>; <sup>1</sup>H NMR (500 MHz, DMSO- $d_6$ ):  $\delta$  8.74 (s, 1H), 8.63 (d,  $J = 6.5$  Hz, 1H), 8.53  
12 (s, 1H), 7.70 (d,  $J = 9.0$  Hz, 1H), 7.56 (d,  $J = 9.0$  Hz, 1H), 7.29 (m, 1H), 7.02 (dd,  $J = 9.0, 2.5$   
13 Hz, 1H), 6.91-6.87 (m, 2H), 3.31 (m, 4H), 2.83 (m, 4H).  
14  
15  
16  
17  
18  
19  
20

21  
22 **3-(Imidazo[2,1-b]thiazol-6-yl)-7-(piperazin-1-yl)-2H-chromen-2-one (31).** Compound **31** was  
23 prepared from **6** and 2-aminothiazole by following the procedure used to prepare **8**. LC-MS:  $m/z$   
24 = 353.1 [M+H]<sup>+</sup>. <sup>1</sup>H NMR (500 MHz, DMSO- $d_6$ )  $\delta$  8.53 (s, 1H), 8.31 (s, 1H), 7.95 (d,  $J = 4.4$   
25 Hz, 1H), 7.64 (d,  $J = 8.8$  Hz, 1H), 7.26 (d,  $J = 4.4$  Hz, 1H), 7.01 (dd,  $J = 8.8, 2.5$  Hz, 1H), 6.85  
26 (d,  $J = 2.2$  Hz, 1H), 3.28 (m, 4H), 2.83 (m, 4H).  
27  
28  
29  
30  
31  
32  
33

34  
35 **3-(6-Methylimidazo[1,2-a]pyridin-2-yl)-7-(piperazin-1-yl)-2H-chromen-2-one (32).**

36  
37 Compound **32** was prepared from **6** and 2-amino-5-methylpyridine by following the procedure  
38 used to prepare **8**. LC-MS:  $m/z = 361.2$  [M+H]<sup>+</sup>. <sup>1</sup>H NMR (500 MHz, DMSO- $d_6$ ):  $\delta$  8.71 (s, 1H),  
39 8.43 (s, 2H), 7.71 (d,  $J = 8.5$  Hz, 1H), 7.46 (d,  $J = 9.5$  Hz, 1H), 7.15 (dd,  $J = 9.0, 1.5$  Hz, 1H), 7.04  
40 (dd,  $J = 9.0, 2.5$  Hz, 1H), 6.91 (d,  $J = 2.0$  Hz, 1H), 3.40-3.35 (m, 4H), 2.97-2.95 (m, 4H), 2.29 (s,  
41 3H).  
42  
43  
44  
45  
46  
47  
48

49  
50 **3-(6-Ethylimidazo[1,2-a]pyridin-2-yl)-7-(piperazin-1-yl)-2H-chromen-2-one (33).** Compound  
51 **33** was prepared from **6** and 2-amino-5-ethylpyridine by following the procedure used to prepare  
52 **8**. LC-MS:  $m/z = 375.3$  [M+H]<sup>+</sup>. <sup>1</sup>H NMR (500 MHz, DMSO- $d_6$ ):  $\delta$  8.80 (s, 1H), 8.54 (s, 2H),  
53 7.78 (d,  $J = 9.0$  Hz, 1H), 7.58 (d,  $J = 9.5$  Hz, 1H), 7.30 (dd,  $J = 9.0, 1.5$  Hz, 1H), 7.11 (dd,  $J =$   
54  
55  
56  
57  
58  
59  
60

1  
2  
3 9.0, 2.5 Hz, 1H), 6.96 (d,  $J = 2.0$  Hz, 1H), 3.40 (m, 4H), 2.93 (m, 4H), 2.71 (q,  $J = 7.5$  Hz, 2H),  
4  
5 1.33 (t,  $J = 7.5$  Hz, 3H).  
6  
7

8  
9 **3-(6-Methylimidazo[1,2-a]pyrazin-2-yl)-7-(piperazin-1-yl)-2H-chromen-2-one (35).**

10  
11 Compound **35** was prepared from **6** and 2-amino-5-methylpyrazine by following the procedure  
12 used to prepare **8**. LC-MS:  $m/z = 362.2$   $[M+H]^+$ .  $^1\text{H NMR}$  (500 MHz, DMSO- $d_6$ )  $\delta$  8.97 (s, 1H),  
13 8.79 (s, 1H), 8.57 (m, 1H), 8.48 (m, 1H), 7.74 (d,  $J = 9.1$  Hz, 1H), 7.05 (dd,  $J = 9.0, 2.4$  Hz, 1H),  
14 6.92 (d,  $J = 2.2$  Hz, 1H), 3.44 (m, 4H), 2.97 (m, 4H), 2.43 (s, 3H).  
15  
16  
17  
18  
19  
20

21  
22 **3-(6,8-Dimethylimidazo[1,2-a]pyrazin-2-yl)-7-(piperazin-1-yl)-2H-chromen-2-one (36).**

23  
24 Compound **36** was prepared from **7** following the procedure used to prepare **8**. LC-MS:  $m/z =$   
25 376.3  $[M+H]^+$ .  $^1\text{H NMR}$  (500 MHz, DMSO- $d_6$ )  $\delta$  8.73 (s, 1H), 8.52 (s, 1H), 8.32 (s, 1H), 7.75 (d,  
26  $J = 9.1$  Hz, 1H), 7.02 (dd,  $J = 9.0, 2.4$  Hz, 1H), 6.86 (d,  $J = 2.2$  Hz, 1H), 3.31 (m, 4H), 2.83 (m,  
27 4H), 2.76 (s, 3H), 2.37 (s, 3H).  
28  
29  
30  
31  
32  
33

34  
35 **3-(8-Ethyl-6-methylimidazo[1,2-a]pyrazin-2-yl)-7-(piperazin-1-yl)-2H-chromen-2-one (37).**

36  
37 Compound **37** was prepared from **6** and 2-amino-3-ethyl-5-methylpyrazine by following the  
38 procedure used to prepare **8**. LC-MS:  $m/z = 390.3$   $[M+H]^+$ .  $^1\text{H NMR}$  (500 MHz, methanol- $d_4$ )  $\delta$   
39 8.65 (s, 1H), 8.39 (s, 1H), 7.96 (s, 1H), 7.53 (d,  $J = 8.5$  Hz, 1H), 6.92 (d,  $J = 8.8$  Hz, 1H), 6.77 (s,  
40 1H), 3.44-3.37 (4H), 3.17 (q,  $J = 7.5$  Hz, 2H), 3.10-3.02 (4H), 2.38 (s, 3H), 1.37 (t,  $J = 7.6$  Hz,  
41 3H).  
42  
43  
44  
45  
46  
47  
48  
49

50  
51 **(R)-3-(6,8-dimethylimidazo[1,2-a]pyrazin-2-yl)-7-(3-methylpiperazin-1-yl)-2H-chromen-2-**  
52 **one (43).** Compound **43** was prepared from **7** and (*R*)-2-methylpiperazine by following the  
53 procedure used to prepare **8**. LC-MS:  $m/z = 390.2$   $[M+H]^+$ .  $^1\text{H NMR}$  (500 MHz, CDCl<sub>3</sub>)  $\delta$  8.74

54  
55 (s, 1H), 8.45 (s, 1H), 7.77 (s, 1H), 7.51 (d,  $J = 8.8$  Hz, 1H), 6.88 (dd,  $J = 8.8$  Hz, 2.5 Hz, 1H),  
56  
57  
58  
59  
60

6.77 (d,  $J = 2.5$  Hz, 1H), 3.77-3.67 (m, 2H), 3.21-3.14 (m, 2H), 3.06-2.92 (m, 3H), 2.91 (s, 3H), 2.60 (m, 1H), 2.48 (s, 3H), 1.20 (d,  $J = 6.3$  Hz, 3H).

**(S)-3-(6,8-Dimethylimidazo[1,2-a]pyrazin-2-yl)-7-(3-isopropylpiperazin-1-yl)-2H-chromen-2-one (44).** Compound **44** was prepared from **7** and (*S*)-2-isopropylpiperazine by following the procedure used to prepare **8**. LC-MS:  $m/z = 418.2$   $[M+H]^+$ .  $^1H$  NMR (500 MHz, methanol- $d_4$ )  $\delta$  8.52 (s, 1H), 8.33 (s, 1H), 8.00 (s, 1H), 7.43 (d,  $J = 8.8$  Hz, 1H), 6.87 (m, 1H), 6.67 (d,  $J = 2.2$  Hz, 1H) 3.76 (m, 2H), 3.04 (m, 1H), 2.81 (m, 2H), 2.71 (s, 3H), 2.55 (m, 1H) 2.43 (m, 1H), 2.30 (s, 3H), 1.63 (m, 1H), 0.96 (d,  $J = 6.6$  Hz, 6H).

**3-(6,8-Dimethylimidazo[1,2-a]pyrazin-2-yl)-7-((3aR,6aS)-hexahydropyrrolo[3,4-c]pyrrol-2(1H)-yl)-2H-chromen-2-one (45).** Compound **45** was prepared from **7** and (3a*S*,6a*S*)-octahydropyrrolo[3,4-*c*]pyrrole by following the procedure used to prepare **8**. LC-MS:  $m/z = 402.1$   $[M+H]^+$ .  $^1H$  NMR (500 MHz, DMSO- $d_6$ )  $\delta$  8.71 (s, 1H), 8.49 (s, 1H), 8.31 (s, 1H), 7.72 (d,  $J = 8.5$  Hz, 1H), 6.68 (dd,  $J = 8.5$  Hz, 2.0 Hz, 1H), 6.51 (d,  $J = 2.0$  Hz, 1H), 3.61 (m, 2H), 3.22 (dd,  $J = 10.5$ , 3.5 Hz, 2H), 2.96 (m, 2H), 2.89 (m, 2H), 2.76 (s, 3H), 2.69 (dd,  $J = 10.5$ , 2.5 Hz, 2H), 2.37 (s, 3H).

**3-(6,8-Dimethylimidazo[1,2-a]pyrazin-2-yl)-7-((3aS,6aS)-hexahydropyrrolo[3,4-b]pyrrol-1(2H)-yl)-2H-chromen-2-one (46).** Compound **46** was prepared from **7** and (3a*S*,6a*S*)-octahydropyrrolo[3,4-*b*]pyrrole by following the procedure used to prepare **8**. LC-MS:  $m/z = 402.1$   $[M+H]^+$ .  $^1H$  NMR (500 MHz, DMSO- $d_6$ )  $\delta$  8.71 (s, 1H), 8.49 (s, 1H), 8.31 (s, 1H), 7.72 (d,  $J = 11.0$  Hz, 1H), 6.65 (dd,  $J = 11.0$ , 2.5 Hz, 1H), 6.48 (d,  $J = 2.5$  Hz, 1H), 4.18 (m, 1H), 3.53 (m, 1H), 3.40 (m, 1H), 3.01 (dd,  $J = 12.0$ , 6.0 Hz, 1H), 2.87 (m, 2H), 2.76 (s, 3H), 2.74 (m, 1H), 2.69 (m, 1H), 2.37 (s, 3H), 2.11 (m, 1H), 1.84 (m, 1H).

1  
2  
3  
4 **(S)-3-(6,8-Dimethylimidazo[1,2-a]pyrazin-2-yl)-7-(4-(2-fluoroethyl)-3-methylpiperazin-1-**  
5 **yl)-2H-chromen-2-one (47).** A mixture of **8** (40 mg, 0.1 mmol), 1-bromo-2-fluoroethane (16.5  
6 mg, 0.13 mmol) and potassium carbonate (27.6 mg, 0.2 mmol) in DMF (0.2 mL) was stirred at  
7 120 °C for 2 h. The organic volatiles were removed by a stream of nitrogen. The residue was  
8 purified by silica gel chromatography (0-10% MeOH in CH<sub>2</sub>Cl<sub>2</sub>) to provide **47** (36 mg, 80%).  
9  
10 LC-MS:  $m/z = 436.4$  [M+H]<sup>+</sup>. <sup>1</sup>H NMR (500 MHz, methanol-*d*<sub>4</sub>) δ 8.49 (s, 1H), 8.34 (s, 1H),  
11 8.00 (s, 1H), 7.44 (d, *J* = 8.8 Hz, 1H), 6.90 (dd, *J* = 8.8, 2.2 Hz, 1H), 6.68 (d, *J* = 2.2 Hz, 1H),  
12 4.68 (ddd, *J* = 8.1, 6.2, 3.6 Hz, 1H), 4.58 (ddd, *J* = 7.7, 6.4, 3.6 Hz, 1H), 3.69 (m, 2H), 3.23-3.04  
13 (3H), 2.84-2.65 (6H), 2.58 (m, 1H), 2.37 (d, *J* = 1.0 Hz, 3H), 1.20 (d, *J* = 6.0 Hz, 3H).  
14  
15  
16  
17  
18  
19  
20  
21  
22  
23  
24

25 **(S)-3-(6,8-Dimethylimidazo[1,2-a]pyrazin-2-yl)-7-(4-(3-fluoropropyl)-3-methylpiperazin-1-**  
26 **yl)-2H-chromen-2-one (48).** Compound **48** was prepared similarly to **47** by reacting **8** with 1-  
27 fluoro-3-iodopropane at 80 °C (78% yield). LC-MS:  $m/z = 450.4$  [M+H]<sup>+</sup>. <sup>1</sup>H NMR (500 MHz,  
28 methanol-*d*<sub>4</sub>) δ 8.60 (s, 1H), 8.42 (s, 1H), 8.07 (s, 1H), 7.51 (d, *J* = 8.8 Hz, 1H), 6.96 (dd, *J* = 9.0,  
29 2.4 Hz, 1H), 6.76 (d, *J* = 2.2 Hz, 1H), 4.58 (d, *J* = 6.6 Hz, 1H), 4.49 (m, 1H), 3.80-3.67 (2H),  
30 3.17-2.96 (3H), 2.87-2.79 (4H), 2.65 (m, 1H), 2.51 (d, *J* = 9.5 Hz, 2H), 2.41 (d, *J* = 0.6 Hz, 3H),  
31 2.04-1.82 (2H), 1.21 (d, *J* = 6.3 Hz, 3H).  
32  
33  
34  
35  
36  
37  
38  
39  
40  
41  
42

43 **3-(6,8-Dimethylimidazo[1,2-a]pyrazin-2-yl)-7-(4-methylpiperazin-1-yl)-2H-chromen-2-one**  
44 **(49).** Compound **49** was prepared from **7** and 1-methylpiperazine by following the procedure  
45 used to prepare **8**. LC-MS:  $m/z = 390.1$  [M+H]<sup>+</sup>. <sup>1</sup>H NMR (500 MHz, CDCl<sub>3</sub>) δ 8.75 (s, 1H),  
46 8.45 (s, 1H), 7.77 (s, 1H), 7.52 (d, *J* = 8.8 Hz, 1H), 6.89 (dd, *J* = 8.8, 2.5 Hz, 1H), 6.78 (d, *J* =  
47 2.2 Hz, 1H), 3.43 (m, 4H), 2.92 (s, 3H), 2.62 (m, 4H), 2.49 (d, *J* = 0.6 Hz, 3H), 2.40 (s, 3H).  
48  
49  
50  
51  
52  
53  
54  
55  
56  
57  
58  
59  
60

**3-(6,8-Dimethylimidazo[1,2-a]pyrazin-2-yl)-7-(4-ethylpiperazin-1-yl)-2H-chromen-2-one**

**(50).** Compound **50** was prepared from **7** and 1-ethylpiperazine by following the procedure used to prepare **8**. LC-MS:  $m/z = 404.2$   $[M+H]^+$ .  $^1H$  NMR (500 MHz, methanol- $d_4$ )  $\delta$  8.61 (s, 1H), 8.38 (s, 1H), 7.96 (s, 1H), 7.48 (d,  $J = 8.8$  Hz, 1H), 6.90 (dd,  $J = 8.8, 2.2$  Hz, 1H), 6.73 (d,  $J = 2.2$  Hz, 1H), 3.43-3.37 (4H), 2.77 (s, 3H), 2.74-2.65 (4H), 2.56 (q,  $J = 7.3$  Hz, 2H), 2.36 (s, 3H), 1.13 (t,  $J = 7.3$  Hz, 3H).

**7-(4-(tert-Butyl)piperazin-1-yl)-3-(6,8-dimethylimidazo[1,2-a]pyrazin-2-yl)-2H-chromen-2-one (51).**

Compound **51** was prepared from **7** and 1-*tert*-butylpiperazine by following the procedure used to prepare **8**. LC-MS:  $m/z = 432.3$   $[M+H]^+$ .  $^1H$  NMR (500 MHz, DMSO- $d_6$ )  $\delta$  8.75 (s, 1H), 8.53 (s, 1H), 8.33 (s, 1H), 7.77 (d,  $J = 8.8$  Hz, 1H), 7.03 (dd,  $J = 8.8, 2.2$  Hz, 1H), 6.88 (d,  $J = 2.2$  Hz, 1H), 3.39-3.35 (4H), 2.76 (s, 3H), 2.66-2.61 (4H), 2.38 (s, 3H), 1.06 (s, 9H).

**(S)-3-(6,8-Dimethylimidazo[1,2-a]pyrazin-2-yl)-7-(hexahydropyrrolo[1,2-a]pyrazin-2(1H)-yl)-2H-chromen-2-one (52).**

Compound **52** was prepared from **7** and (*S*)-octahydropyrrolo[1,2-a]pyrazine by following the procedure used to prepare **8**. LC-MS:  $m/z = 416.1$   $[M+H]^+$ .  $^1H$  NMR (500 MHz, methanol- $d_4$ )  $\delta$  8.75 (s, 1H), 8.52 (s, 1H), 8.14 (s, 1H), 7.63 (d,  $J = 8.8$  Hz, 1H), 7.05 (dd,  $J = 8.8, 2.2$  Hz, 1H), 6.89 (d,  $J = 2.2$  Hz, 1H), 4.09 (m, 1H), 3.93 (m, 1H), 3.29-3.18 (3H), 2.96 (m, 1H), 2.88 (s, 3H), 2.82-2.59 (3H), 2.47 (s, 3H), 2.13 (m, 1H), 2.00 (m, 2H), 1.69 (m, 1H).

**7-(4-(Dimethylamino)piperidin-1-yl)-3-(6,8-dimethylimidazo[1,2-a]pyrazin-2-yl)-2H-**

**chromen-2-one (53).** Compound **53** was prepared from **7** and *N,N*-dimethylpiperidin-4-amine by following the procedure used to prepare **8**. LC-MS:  $m/z = 418.3$   $[M+H]^+$ ,  $^1H$  NMR (500 MHz, DMSO- $d_6$ )  $\delta$  8.73 (s, 1H), 8.52 (s, 1H), 8.32 (s, 1H), 7.74 (d,  $J = 8.8$  Hz, 1H), 7.03 (dd,  $J = 9.0,$

2.3 Hz, 1H), 6.9 (d,  $J = 2.2$  Hz, 1H), 4.02 (m, 2H), 2.93 (m, 2H), 2.76 (s, 3H), 2.38 (s, 3H), 2.35 (m, 1H), 2.19 (s, 6H), 1.84 (m, 2H), 1.43 (m, 2H).

**3-(6,8-Dimethylimidazo[1,2-a]pyrazin-2-yl)-7-(piperazin-1-yl)-1H-isochromen-1-one (65).**

Compound **65** was prepared from **13** and piperazine by following the procedure used to prepare **14**. LC-MS:  $m/z = 376.3$   $[M+H]^+$ .  $^1H$  NMR (500 MHz, DMSO- $d_6$ )  $\delta$  8.37 (s, 1H), 8.28 (s, 1H), 7.78 (d,  $J = 8.8$  Hz, 1H), 7.69-7.56 (2H), 7.47 (s, 1H), 3.60-3.47 (m, 4H), 3.28-3.21 (m, 4H), 2.74 (s, 3H), 2.39 (d,  $J = 1.0$  Hz, 3H).

**2-(4,6-Dimethylpyrazolo[1,5-a]pyrazin-2-yl)-7-(piperazin-1-yl)-4H-pyrido[1,2-a]pyrimidin-**

**4-one (67).** Compound **67** was prepared from **19** and piperazine by following the procedure used to prepare **20**. LC-MS:  $m/z = 376.5$   $[M+H]^+$ .  $^1H$  NMR (500 MHz, DMSO- $d_6$ )  $\delta$  8.50 (m, 1H), 8.27 (m, 1H), 8.11 (m, 1H), 7.73 (m, 1H), 7.55 (d,  $J = 0.9$  Hz, 1H), 6.96 (s, 1H), 3.18 (m, 4H), 2.92 (m, 4H), 2.73 (s, 3H), 2.43 (s, 3H).

**7-(4-Cyclopropylpiperazin-1-yl)-2-(4,6-dimethylpyrazolo[1,5-a]pyrazin-2-yl)-4H-**

**pyrido[1,2-a]pyrimidin-4-one (69).** Compound **69** was prepared from **19** and 1-

cyclopropylpiperazine by following the procedure used to prepare **20**. LC-MS:  $m/z = 416.4$   $[M+H]^+$ .  $^1H$  NMR (500 MHz, DMSO- $d_6$ )  $\delta$  8.56 (m, 1H), 8.27 (m, 1H), 8.12 (m, 1H), 7.73 (m, 1H), 7.55 (m, 1H), 6.96 (s, 1H), 3.21 (m, 4H), 2.73 (s, 3H), 2.70 (m, 4H), 2.43 (s, 3H), 1.71 (m, 1H), 0.47 (m, 2H), 0.36 (m, 2H).

**(S)-2-(4,6-Dimethylpyrazolo[1,5-a]pyrazin-2-yl)-7-(hexahydropyrrolo[1,2-a]pyrazin-2(1H)-yl)-4H-pyrido[1,2-a]pyrimidin-4-one (71).** Compound **71** was prepared from **19** and (S)-

octahydropyrrolo[1,2-a]pyrazine by following the procedure used to prepare **20**. LC-MS:  $m/z = 416.3$   $[M+H]^+$ .  $^1H$  NMR (500 MHz, DMSO- $d_6$ )  $\delta$  8.56 (m, 1H), 8.29 (m, 1H), 8.15 (m, 1H), 7.73

1  
2  
3 (m, 1H), 7.54 (m, 1H), 6.95 (m, 1H), 3.90 (m, 1H), 3.73 (m, 1H), 3.13 (m, 1H), 3.04 (m, 1H),  
4  
5 2.86 (m, 1H), 2.73 (s, 3H), 2.53 (m, 1H), 2.43 (s, 3H), 2.29 (m, 1H), 2.11 (m, 2H), 1.87 (m, 1H),  
6  
7 1.82-1.65 (2H), 1.41 (m, 1H).  
8  
9

10  
11 **7-(4-(Dimethylamino)piperidin-1-yl)-2-(4,6-dimethylpyrazolo[1,5-a]pyrazin-2-yl)-4H-**

12 **pyrido[1,2-a]pyrimidin-4-one (72).** Compound **72** was prepared from **19** and N,N-

13  
14  
15 dimethylpiperidin-4-amine by following the procedure used to prepare **20**. LC-MS:  $m/z = 418.4$

16  
17 [M+H]<sup>+</sup>. <sup>1</sup>H NMR (500 MHz, DMSO-*d*<sub>6</sub>) δ 8.56 (m, 1H), 8.30 (m, 1H), 8.12 (m, 1H), 7.71 (m,  
18  
19 1H), 7.55 (d,  $J = 1.3$  Hz, 1H), 6.95 (s, 1H), 3.83-3.73 (m, 2H), 2.88-2.78 (m, 2H), 2.73 (s, 3H),  
20  
21 2.43 (s, 3H), 2.28 (m, 1H), 2.23 (br s, 6H), 1.96-1.85 (m, 2H), 1.61-1.46 (m, 2H).  
22  
23  
24  
25

26  
27 **(R)-2-(4,6-Dimethylpyrazolo[1,5-a]pyrazin-2-yl)-7-(3-methylpiperazin-1-yl)-4H-pyrido[1,2-**

28 **a]pyrimidin-4-one (73).** Compound **73** was prepared from **19** and (*R*)-2-methylpiperazine by

29 following the procedure used to prepare **20**. LC-MS:  $m/z = 390.4$  [M+H]<sup>+</sup>. <sup>1</sup>H NMR (500 MHz,  
30  
31 DMSO-*d*<sub>6</sub>) δ 8.55 (d,  $J = 0.6$  Hz, 1H), 8.23 (d,  $J = 2.8$  Hz, 1H), 8.11 (dd,  $J = 9.8, 2.8$  Hz, 1H),  
32  
33 7.70 (d,  $J = 9.5$  Hz, 1H), 7.52 (d,  $J = 0.9$  Hz, 1H), 6.94 (s, 1H), 3.66-3.56 (m, 2H), 3.03 (m, 1H),  
34  
35 2.89-2.78 (m, 2H), 2.73 (s, 3H), 2.69-2.59 (m, 1H), 2.43 (s, 3H), 2.30 (t,  $J = 10.9$  Hz, 1H), 1.07  
36  
37 (d,  $J = 6.7$  Hz, 3H).  
38  
39  
40  
41  
42  
43

44 **(S)-2-(4,6-Dimethylpyrazolo[1,5-a]pyrazin-2-yl)-7-(3-methylpiperazin-1-yl)-4H-pyrido[1,2-**

45 **a]pyrimidin-4-one (74).** Compound **74** was prepared from **19** and (*S*)-2-methylpiperazine by

46 following the procedure used to prepare **20**. LC-MS:  $m/z = 390.5$  [M+H]<sup>+</sup>. <sup>1</sup>H NMR (500 MHz,  
47  
48 DMSO-*d*<sub>6</sub>) δ 8.55 (d,  $J = 0.6$  Hz, 1H), 8.23 (d,  $J = 2.8$  Hz, 1H), 8.11 (dd,  $J = 9.8, 2.8$  Hz, 1H),  
49  
50 7.70 (d,  $J = 9.5$  Hz, 1H), 7.52 (d,  $J = 0.9$  Hz, 1H), 6.94 (s, 1H), 3.66-3.56 (m, 2H), 3.03 (m, 1H),  
51  
52  
53  
54  
55  
56  
57  
58  
59  
60

1  
2  
3 2.89-2.78 (m, 2H), 2.73 (s, 3H), 2.69-2.59 (m, 1H), 2.43 (s, 3 H), 2.30 (t,  $J = 10.9$  Hz, 1H), 1.07  
4  
5  
6 (d,  $J = 6.7$  Hz, 3H).  
7

8  
9 **3-(6-Methylimidazo[1,2-a]pyrazin-2-yl)-7-(4-methylpiperazin-1-yl)-2H-chromen-2-one (75).**

10  
11 Compound **75** was prepared from **6** and 2-amino-5-methylpyrazine by following the procedure  
12 used to prepare **8**. LC-MS:  $m/z = 376.2$   $[M+H]^+$ .  $^1\text{H}$  NMR (500 MHz, DMSO- $d_6$ )  $\delta$  8.98 (s, 1H),  
13  
14 8.79 (s, 1H), 8.57 (s, 1H), 8.49 (t,  $J = 1.1$  Hz, 1H), 7.73 (d,  $J = 9.1$  Hz, 1H), 7.05 (dd,  $J = 9.0, 2.3$   
15  
16 Hz, 1H), 6.91 (d,  $J = 2.2$  Hz, 1H), 3.41 (br s, 4H), 2.47 (br s, 4H), 2.43 (d,  $J = 0.6$  Hz, 3H), 2.25  
17  
18 (s, 3H).  
19  
20  
21

22  
23  
24 **(S)-3-(6,8-Dimethylimidazo[1,2-a]pyrazin-2-yl)-7-(3,4-dimethylpiperazin-1-yl)-2H-**

25  
26 **chromen-2-one (76).** Compound **76** was prepared according to the procedure for **9**. LC-MS:  $m/z$   
27  
28 = 404.1  $[M+H]^+$ .  $^1\text{H}$  NMR (500 MHz, DMSO- $d_6$ )  $\delta$  8.71 (s, 1H), 8.51 (s, 1H), 8.31 (s, 1H), 7.75  
29  
30 (d,  $J = 8.8$  Hz, 1H), 7.04 (dd,  $J = 8.8, 2.2$  Hz, 1H), 6.89 (d,  $J = 2.2$  Hz, 1H), 3.83 (m, 2H), 2.97  
31  
32 (m, 1H), 2.83 (m, 1H), 2.75 (s, 3H), 2.59 (m, 1H), 2.36 (s, 3H), 2.21 (s, 3H), 2.19 (m, 1H), 2.11  
33  
34 (m, 1H), 1.07 (d,  $J = 6.3$  Hz, 3H).  
35  
36  
37  
38

39  
40 **3-(6-Methylimidazo[1,2-a]pyrazin-2-yl)-7-(4-methylpiperazin-1-yl)-1H-isochromen-1-one**

41  
42 **(77).** Compound **77** was prepared from **12** and 2-amino-5-methylpyrazine by following the  
43 procedure used to prepare **14**. LC-MS:  $m/z = 376.2$   $[M+H]^+$ .  $^1\text{H}$  NMR (500 MHz,  $\text{CDCl}_3$ )  $\delta$  9.04  
44  
45 (s, 1H), 8.06 (s, 1H), 7.93 (s, 1H), 7.75 (d,  $J = 2.5$  Hz, 1H), 7.49 (d,  $J = 8.5$  Hz, 1H), 7.41 (s, 1H),  
46  
47 7.38 (dd,  $J = 8.5, 2.5$  Hz, 1H), 3.44-3.37 (4H), 2.68-2.61 (4H), 2.57 (s, 3H), 2.41 (s, 3H).  
48  
49  
50  
51

52 **SMN2 minigene luciferase reporter assay in cultured cells.** The methods and conditions  
53 utilized to perform the luciferase assay in HEK293H cells (ATCC) were described previously.<sup>17</sup>  
54  
55  
56  
57  
58  
59  
60

1  
2  
3 **RT-qPCR analysis of full length *SMN2* minigene mRNA.** HEK293H cells stably transfected  
4 with the *SMN2* minigene (*SMN2mg*) reporter construct<sup>17</sup> were plated at a density of 10,000  
5 cells/well in 200  $\mu$ l Dulbecco's Modified Eagle's Medium (DMEM) with GlutaMAX, 10% fetal  
6 bovine serum (FBS) and 200  $\mu$ g/mL hygromycin (Life Technologies, Inc.) in 96-well plates, and  
7 incubated for 6 hours in a cell culture incubator (37 °C, 5% CO<sub>2</sub>, 100% relative humidity). Cells  
8 were then treated with compound at different concentrations (0.5% DMSO) in duplicate for 24  
9 hours. After removal of the supernatant, cells were lysed in Cells-To-Ct lysis buffer (Life  
10 Technologies, Inc.) according to the manufacturer's recommendations. The mRNA levels of full  
11 length *SMN2* minigene and *GAPDH* were quantified using Taqman-based RT-qPCR and *SMN2*  
12 minigene-specific primers and probes in Table 1 of the supporting information (purchased from  
13 Life Technologies, Inc.). The *SMN2* minigene forward and reverse primers were each used at a  
14 final concentration of 0.4  $\mu$ M. The *SMN2* minigene probe was used at a final concentration of  
15 0.15  $\mu$ M. *GAPDH* primers were used at final concentrations of 0.2  $\mu$ M and the probe at 0.15  $\mu$ M.  
16 RT-qPCR was carried out at the following temperatures for indicated times: Step 1: 48 °C (15  
17 min); Step 2: 95 °C (10 min); Step 3: 95 °C (15 sec); Step 4: 60 °C (1 min); Steps 3 and 4 were  
18 repeated for 40 cycles. The Ct values for each mRNA were converted to mRNA abundance using  
19 actual PCR efficiencies. Full length *SMN2* minigene mRNA was normalized to *GAPDH* and  
20 DMSO controls and plotted as fold change compared to DMSO treatment.  
21  
22  
23  
24  
25  
26  
27  
28  
29  
30  
31  
32  
33  
34  
35  
36  
37  
38  
39  
40  
41  
42  
43  
44  
45

46 **SMN protein assay in cultured cells.** The methods and conditions utilized to perform the HTRF  
47 assay in patient fibroblasts GM03813 (Coriell Institute) were described previously.<sup>17</sup>  
48  
49  
50  
51

52 **SMN protein in tissues of neonatal  $\Delta$ 7 SMA mice.** The SMA  $\Delta$ 7 homozygous knockout mice  
53 (FVB.Cg-Tg(*SMN2*\* $\Delta$ 7)4299Ahmb Tg(*SMN2*)89Ahmb *Smn1tm1Msd/J*, Jackson  
54 Laboratory) were dosed once a day (QD) intraperitoneally (IP) with a test compound or vehicle  
55  
56  
57  
58  
59  
60

1  
2  
3 (100% DMSO) from postnatal day (PND) 3 to day 9. Tissues were collected for analysis of  
4  
5 SMN protein levels. The tissue samples in Safe-Lock tubes (Eppendorf) were weighed and the  
6  
7 volume of RIPA buffer (20 mM Tris-HCl pH 7.5, 150 mM NaCl, 1 mM EDTA, 1% NP 40, 1%  
8  
9 Sodium deoxycholate) containing the protease inhibitor cocktail (Roche Applied Science) was  
10  
11 added based on the weight to volume ratios for each type of tissue: Brain (50 mg/mL), Muscle  
12  
13 (50 mg/mL) and Spinal Cord (25 mg/mL). Tissues were homogenized using the TissueLyzer  
14  
15 (Qiagen) by bead milling. 5 mm stainless steel beads were added to the sample and shaken  
16  
17 vigorously for 5 minutes at 30 Hz in the TissueLyzer. The samples were then centrifuged for 20  
18  
19 minutes at 14,000 x g in a microcentrifuge and the homogenates transferred to the PCR plate.  
20  
21  
22 The homogenates were diluted in RIPA buffer to approximately 1 mg/mL for HTRF and  
23  
24 approximately 0.5 mg/mL for total protein measurement using the BCA protein assay (kit  
25  
26 available from Pierce). For the SMN HTRF assay, 35  $\mu$ L of the tissue homogenate were  
27  
28 transferred to a 384 well plate containing 5  $\mu$ L of the antibody solution (1:100 dilution of each of  
29  
30 the anti-SMN<sub>2</sub> [Cisbio] and anti-SMN Kryptate [Cisbio] in reconstitution buffer). The plate  
31  
32 was centrifuged for 1 minute to bring the solution to the bottom of the wells, then incubated  
33  
34 overnight at rt. Fluorescence for each well of the plate at 665 nm and 620 nm was measured on  
35  
36 an EnVision multilabel plate reader (Perkin Elmer). The total SMN protein in the tissue  
37  
38 homogenate was measured using the BCA assay according to the manufacturer's protocol. The  
39  
40 total protein normalized change in SMN protein signal for each test compound and vehicle  
41  
42 treated tissue sample was calculated as the percent difference in the signal in the presence of the  
43  
44 test compound and the signal in the absence of the test compound (vehicle control) divided by  
45  
46 the signal in the absence of the test compound.  
47  
48  
49  
50  
51  
52  
53  
54  
55  
56  
57  
58  
59  
60

1  
2  
3 **Survival of neonatal  $\Delta 7$  SMA mice.** SMA  $\Delta 7$  homozygous knockout mice (FVB.Cg-  
4 Tg(SMN2\*delta7)4299Ahmb Tg(SMN2)89Ahmb Smn1tm1Msd/J, Jackson Laboratory) were  
5  
6 dosed intraperitoneally (IP) with test compound or vehicle (100% DMSO) once per day (QD)  
7  
8 from postnatal day (PND) 3 until the dose regimen was switched to an oral dose twice per day  
9  
10 (BID) in 0.5% hydroxypropylmethyl cellulose (HPMC) with 0.1% Tween-80 at a dose 3.16-fold  
11  
12 higher than the dose used for IP. The number of surviving mice in each group was recorded  
13  
14 every day and plotted as a percent of total number of mice.  
15  
16  
17  
18  
19  
20

## 21 **SUPPORTING INFORMATION**

22  
23  
24 Experimental details on the synthesis and characterization of building blocks **1b** and **1c**, and the  
25  
26 target compounds **34**, **38-42**, **54-64**, **66**, **68**, **70** and **78** can be found in the supporting information  
27  
28 provided. This material is available free of charge via the Internet at <http://pubs.acs.org>.  
29  
30  
31

## 32 **AUTHOR INFORMATION**

33  
34  
35  
36 Corresponding Author. \*E-mail: [gkarp@ptcbio.com](mailto:gkarp@ptcbio.com). Phone: (908)-912-9144.  
37  
38

## 39 **ACKNOWLEDGEMENTS**

40  
41  
42 We acknowledge Drs. Sergey Paushkin, Karen Chen and Michael Pleiss for helpful discussions.  
43  
44 We also acknowledge the SMA Foundation for providing funding to support the research  
45  
46 presented in this paper.  
47  
48  
49

## 50 **REFERENCES**

- 51  
52  
53  
54 1. Lefebvre, S; Bürglen, L.; Reboullet, S.; Clermont, O.; Burlet, P.; Viollet, L.; Benichou,  
55  
56 B.; Cruaud, C.; Millasseau, P.; Zeviani, M.; Paslier, D. L.; Frézal, J.; Cohen, D.;  
57  
58  
59  
60

- 1  
2  
3 Weissenbach, J.; Munnich, A.; Melki, J. Identification and characterization of a spinal  
4 muscular atrophy-determining gene. *Cell* **1995**, *80*, 155-165.  
5  
6  
7  
8 2. Lorson, C. L.; Hahnen, E.; Androphy, J.; Wirth, B. A single nucleotide in the *SMN* gene  
9 regulates splicing and is responsible for spinal muscular atrophy. *Proc. Natl. Acad. Sci.*  
10 *U.S.A.* **1999**, *96*, 6307-6311.  
11  
12  
13  
14  
15 3. Cho, S.; Dreyfuss, G. A degron created by *SMN2* exon 7 skipping is a principal  
16 contributor to spinal muscular atrophy severity. *Genes Dev.* **2010**, *24*, 438-442.  
17  
18  
19  
20 4. Burnett, B. G.; Muñoz E.; Tandon, A.; Kwon, D. Y.; Sumner, C. J.; Fischbeck, K. H.  
21 Regulation of SMN protein stability. *Mol. Cell. Biol.* **2009**, *29*, 1107-1115.  
22  
23  
24  
25 5. Hua, Y.; Vickers, T. A.; Okunola, H. L.; Bennett, C. F.; Krainer, A. R. Antisense  
26 masking of an hnRNP A1/A2 intronic splicing silencer corrects *SMN2* splicing in  
27 transgenic mice. *Am. J. Hum. Genet.* **2008**, *82*, 834-848.  
28  
29  
30  
31  
32 6. Lim, S. R.; Hertel, K. J. Modulation of survival motor neuron pre-mRNA splicing by  
33 inhibition of alternative 3' splice site pairing. *J. Biol. Chem* **2001**, *276*, 45476-45483.  
34  
35  
36  
37 7. Porensky, P. N.; Mitrpant, C.; McGovern, V. L.; Bevan, A. K.; Foust, K. D.; Kaspar, B.  
38 K.; Wilton, S. D.; Burghes, A. H. M. A single administration of morpholino antisense  
39 oligomer rescues spinal muscular atrophy in mouse. *Hum. Mol. Genet.* **2012**, *21*, 1625-  
40 1638.  
41  
42  
43  
44  
45 8. Passini, M. A.; Bu, J.; Richards, A. M.; Kinnecom, C.; Sardi, S. P.; Stanek, L. M.; Hua,  
46 Y.; Rigo, F.; Matson, J.; Hung, G.; Kaye, E. M.; Shihabuddin, L. S.; Krainer, A. R.;  
47 Bennett, C. F.; Cheng, S. H. Antisense oligonucleotides delivered to the mouse CNS  
48 ameliorate symptoms of severe spinal muscular atrophy. *Sci. Transl. Med.* **2011**, *3*, 1-11.  
49  
50  
51  
52  
53  
54  
55  
56  
57  
58  
59  
60

- 1  
2  
3  
4  
5  
6  
7  
8  
9  
10  
11  
12  
13  
14  
15  
16  
17  
18  
19  
20  
21  
22  
23  
24  
25  
26  
27  
28  
29  
30  
31  
32  
33  
34  
35  
36  
37  
38  
39  
40  
41  
42  
43  
44  
45  
46  
47  
48  
49  
50  
51  
52  
53  
54  
55  
56  
57  
58  
59  
60
9. Hua, Y.; Sahashi, K.; Rigo, F.; Hung, G.; Horev, G.; Bennett, C. F.; Krainer, A. R. Peripheral SMN restoration is essential for long-term rescue of a severe spinal muscular atrophy mouse model. *Nature* **2011**, *478*, 123-126.
10. Porensky, P. N.; Mitrpant, C.; McGovern, V. L.; Bevan, A. K.; Foust, K. D.; Kaspar, B. K.; Wilton, S. D.; Burghes, A. H. M. A single administration of morpholino antisense oligomer rescues spinal muscular atrophy in mouse. *Hum. Mol. Genet.* **2012**, *21*, 1625-1638.
11. Zhou, H.; Janghra, N.; Mitrpant, C.; Dickinson, R. L.; Anthony, K.; Price, L.; Eperon, I. C.; Wilton, S. D.; Morgan, J.; Muntoni, F. A novel morpholino oligomer targeting ISS-N1 improves rescue of severe spinal muscular atrophy transgenic mice. *Hum. Gene Ther.* **2013**, *24*, 331-342.
12. Mitrpant, C.; Porensky, P.; Zhou, H.; Price, L.; Muntoni, F.; Fletcher, S.; Wilton, S. D.; Burghes, A. H. M. Improved antisense oligonucleotide design to suppress aberrant *SMN2* gene transcript processing: Towards a treatment for spinal muscular atrophy. *PLoS ONE* **2013**, *8*, e62114.
13. Osman, E. Y.; Miller, M. R.; Robbins, K. L.; Lombardi, A. M.; Atkinson, A. K.; Brehm, A. J.; Lorson, C. L. Morpholino antisense oligonucleotides targeting intronic repressor Element1 improve phenotype in SMA mouse models. *Hum. Mol. Genet.* **2014**, *23*, 4832-4845.
14. Grzeschik, S. M.; Ganta, M.; Prior, T. W.; Heavlin, W. D.; Wang, C. H. Hydroxyurea enhances *SMN2* gene expression in spinal muscular atrophy cells. *Ann. Neurol.* **2005**, *58*, 194-202.

- 1  
2  
3  
4  
5  
6  
7  
8  
9  
10  
11  
12  
13  
14  
15  
16  
17  
18  
19  
20  
21  
22  
23  
24  
25  
26  
27  
28  
29  
30  
31  
32  
33  
34  
35  
36  
37  
38  
39  
40  
41  
42  
43  
44  
45  
46  
47  
48  
49  
50  
51  
52  
53  
54  
55  
56  
57  
58  
59  
60
15. Angelozzi, C.; Borgo, F.; Tiziano, F. D.; Martella, A.; Neri, G.; Brahe, C. Salbutamol increases *SMN* mRNA and protein levels in spinal muscular atrophy cells. *J. Med. Genet.* **2008**, *45*, 29-31.
16. Hastings, M. L.; Berniac, J.; Liu, Y. H.; Abato, P.; Jodelka, F. M.; Barthel, L.; Kumar, S.; Dudley, C.; Nelson, M.; Larson, K.; Edmonds, J.; Bowser, T.; Draper, M; Higgins, P.; Krainer A. R. Tetracyclines that promote *SMN2* exon 7 splicing as therapeutics for spinal muscular atrophy. *Sci. Transl. Med.* **2009**, *1*, 5-12.
17. Chang, J.-G.; Hsieh-Li, H.-M.; Jong, Y.-J.; Wang, N. M.; Tsai, C.-H.; Li, H. Treatment of spinal muscular atrophy by sodium butyrate. *Proc. Natl. Acad. Sci. U.S.A.* **2001**, *98*, 9808-9813.
18. Andreassi, C.; Angelozzi, C.; Tiziano, F. D.; Vitali, T.; De Vincenzi, E.; Boninsegna, A.; Villanova, M.; Bertini, E.; Pini, A.; Neri, G.; Brahe, C. Phenylbutyrate increases *SMN* expression in vitro: relevance for treatment of spinal muscular atrophy. *Eur. J. Hum. Genet.* **2004**, *12*, 59-65.
19. Sumner, C. J.; Huynh, T. N.; Markowitz, J. A.; Perhac, J. S.; Hill, B.; Coover, D. D.; Schussler, K.; Chen, X.; Jarecki, J.; Burghes, A. H. M.; Taylor, J. P.; Fischbeck, K. H. Valproic acid increases *SMN* levels in spinal muscular atrophy patient cells. *Ann. Neurol.* **2003**, *54*, 647-654.
20. Avila, A. M.; Burnett, B. G.; Taye, A. A.; Gabanella, F.; Knight, M. A.; Hartenstein, P.; Cizman, Z.; Di Prospero, N. A.; Pellizzoni, L.; Fischbeck, K. H.; Sumner, C. J. Trichostatin A increases *SMN* expression and survival in a mouse model of spinal muscular atrophy. *J. Clin. Invest.* **2007**, *117*, 659-671.

- 1  
2  
3  
4  
5  
6  
7  
8  
9  
10  
11  
12  
13  
14  
15  
16  
17  
18  
19  
20  
21  
22  
23  
24  
25  
26  
27  
28  
29  
30  
31  
32  
33  
34  
35  
36  
37  
38  
39  
40  
41  
42  
43  
44  
45  
46  
47  
48  
49  
50  
51  
52  
53  
54  
55  
56  
57  
58  
59  
60
21. Naryshkin, N. A.; Weetall, M.; Dakka, A.; Narasimhan, J.; Zhao, X.; Feng, Z.; Ling, K. K. Y.; Karp, G. M.; Qi, H.; Woll, M. G.; Chen, G.; Zhang, N.; Gabbeta, V.; Vazirani, P.; Bhattacharyya, A.; Furia, B.; Risher, N.; Sheedy, J.; Kong, R.; Ma, J.; Turpoff, A.; Lee, C. S.; Zhang, X.; Moon, Y.-C.; Trifillis, P.; Welch, E. M.; Colacino, J. M.; Babiak, J.; Almstead, N. G.; Peltz, S. W.; Eng, L. A.; Chen, K. S.; Mull, J. L.; Lynes, M. S.; Rubin, L. L.; Fontoura, P.; Santarelli, L.; Haehnke, D.; McCarthy, K. D.; Schmucki, R.; Ebeling, M.; Sivaramakrishnan, M.; Ko, C.-P.; Paushkin, S. V.; Ratni, H.; Gerlach, I.; Ghosh, A.; Metzger, F. *SMN2* splicing modifiers improve motor function and longevity in mice with spinal muscular atrophy. *Science* **2014**, *345*, 688-693.
22. Palacino, J.; Swalley, S. E.; Song, C.; Cheung, A. K.; Shu, L.; Zhang, X.; Van Hoosear, M.; Shin, Y.; Chin, D. N.; Keller, C. G.; Martin Beibel, M.; Renaud, N. A.; Smith, T. A.; Salcius, M.; Shi, X.; Hild, M.; Servais, R.; Jain, M.; Deng, L.; Bullock, C.; McLellan, M.; Schuierer, S.; Murphy, L.; Blommers, M. J. J.; Blaustein, C.; Berenshteyn, F.; Lacoste, A.; Thomas, J. R.; Roma, G.; Michaud, G. A.; Tseng, B. S.; Porter, J. A.; Myer, V. E.; Tallarico, J. A.; Hamann, L. G.; Curtis, D.; Fishman, M. C.; Dietrich, W. F.; Dales, N. A.; Sivasankaran R. *SMN2* splice modulators enhance U1-pre-mRNA association and rescue SMA mice. *Nat. Chem. Biol.* **2015**, *11*, 511-517.
23. Achieving a 1.5-fold increase of *SMN2-FL* mRNA in fibroblasts derived from SMA patients is more challenging than achieving a similar increase in HEK293H cells containing the *SMN2* minigene construct, since, as mentioned above, the theoretical maximum increase possible in patient-derived fibroblasts is ~2-fold as opposed to 30-fold in the minigene construct. While early optimization efforts were informed by data from the more sensitive minigene PCR assay, in later efforts, we placed greater weight on

1  
2  
3 the activity observed in patient-derived cells as the potency of the analogs improved. In  
4 patient-derived cells, both the levels of endogenous *SMN2-FL* mRNA and SMN protein  
5 increased in a dose dependent manner in the presence of optimized compounds.  
6  
7

8  
9  
10 However, we chose to utilize the SMN protein EC<sub>1.5X PRO</sub> as the metric for optimization,  
11 since increased SMN protein production is the ultimate desired outcome and it is  
12 dependent on increased levels of functional full length *SMN2* mRNA.  
13  
14

- 15  
16  
17 24. The EC<sub>1.5X RNA</sub> values obtained for 7-piperazinyl coumarins were largely unaffected by  
18 GAPDH correction. Thus, we chose to report the GAPDH corrected values in all  
19 subsequent tables.  
20  
21  
22 25. The pK<sub>a</sub> values were calculated using Advanced Chemistry Development (ACD 12.0)  
23 software.  
24  
25  
26 26. Lee, S.; Sivakumar, K.; Shin, W.-S.; Xie F.; Wang, Q. Synthesis and anti-angiogenesis  
27 activity of coumarin derivatives. *Bioorg. Med. Chem. Lett.* **2006**, *16*, 4596–4599.  
28  
29  
30 27. Auberson, Y. Coumarines useful as biomarkers. WO 2003074519 A1, September 12,  
31 2003.  
32  
33  
34 28. Wu, Q.; Christensen, L. A.; Legerski, R. J.; Vasquez, K. M. Mismatch repair participates  
35 in error-free processing of DNA interstrand crosslinks in human cells. *EMBO Rep.* **2005**,  
36 *6*, 551-556.  
37  
38  
39 29. Le, T. T.; Pham, L.T.; Butchbach, M. E. R.; Zhang, H. L.; Monani, U. R.; Coover, D. D.;  
40 Gavrilina, T. O.; Xing, L.; Bassell, G. J.; Burghes, A. H. M. SMN $\Delta$ 7, the major product  
41 of the centromeric survival motor neuron (*SMN2*) gene, extends survival in mice with  
42 spinal muscular atrophy and associates with full-length SMN. *Hum. Mol. Genet.* **2005**,  
43 *14*, 845-857.  
44  
45  
46  
47  
48  
49  
50  
51  
52  
53  
54  
55  
56  
57  
58  
59  
60

- 1  
2  
3  
4 30. For additional data from survival studies, including body weight and righting reflex  
5 testing for compound **9** see reference 21.  
6  
7  
8 31. For additional data from survival studies, including body weight and righting reflex  
9 testing for compound **14** see: Zhao, X.; Feng, Z.; Ling, K. K. Y; Mollin, A.; Sheedy, J.;  
10 Yeh, S.; Petruska, J.; Narasimhan, J.; Dakka, A.; Welch, E. M.; Karp, G.; Chen, K. S.;  
11 Metzger, F.; Ratni, H.; Lotti, F.; Tisdale, S.; Naryshkin, N. A.; Pellizzoni, L.; Paushkin,  
12 S.; Ko, C.-P.; Weetall, M. Pharmacokinetics, pharmacodynamics, and efficacy of a small-  
13 molecule *SMN2* splicing modifier in mouse models of spinal muscular atrophy. *Hum.*  
14 *Mol. Genet.* [Online early access]. DOI 10.1093/hmg/ddw062. Published online: Feb. 29,  
15 2016  
16  
17  
18  
19  
20  
21  
22  
23  
24  
25  
26  
27 32. For additional data from survival studies, including body weight and righting reflex  
28 testing for compound **20** see supporting information.  
29  
30  
31  
32  
33  
34  
35  
36  
37  
38  
39  
40  
41  
42  
43  
44  
45  
46  
47  
48  
49  
50  
51  
52  
53  
54  
55  
56  
57  
58  
59  
60

1  
2  
3  
4  
5  
6  
7  
8  
9  
10  
11  
12  
13  
14  
15  
16  
17  
18  
19  
20  
21  
22  
23  
24  
25  
26  
27  
28  
29  
30  
31  
32  
33  
34  
35  
36  
37  
38  
39  
40  
41  
42  
43  
44  
45  
46  
47  
48  
49  
50  
51  
52  
53  
54  
55  
56  
57  
58  
59  
60

Table of contents graphic:

